Assessing the impact of different carbonate system parameters on benthic foraminifera from controlled growth experiments

M. Mojtahid [a,*], P. Depuydt [a], A. Mouret [a], S. Le Houedec [a,b], S. Fiorini [c], S. Chollet [c], F. Massol [c], F. Dohou [c], H.L. Filipsson [d], W. Boer [e], G.-J. Reichart [e,f], C. Barras [a]

[a] Univ Angers, Univ Nantes, Univ Le Mans, CNRS, LPG, Laboratoire de Planétologie et Géosciences, UMR 6112, 2 Bd Lavoisier, 49045 Angers Cedex, France
[b] Department of Earth Sciences, University of Geneva, 13 rue des Maraichers, Genève, Switzerland
[c] Centre de recherche en écologie expérimentale et prédictive (CEREEP-Ecotron IleDeFrance), Ecole normale supérieure, CNRS, PSL Research University, UAR 3194, France
[d] Department of Geology, Lund University, Lund, Sweden
[e] Dept. of Ocean Sciences, Royal Netherlands Institute for Sea Research (NIOZ), Texel, the Netherlands
[f] Dept. of Earth Sciences, Faculty of Geosciences, Utrecht University, the Netherlands

ARTICLE INFO

ABSTRACT

Insights into past marine carbon cycling and water mass properties can be obtained by means of geochemical proxies calibrated through controlled laboratory experiments with accurate seawater carbonate system (C-system) manipulations. Here, we explored the use of strontium/calcium ratio (Sr/Ca) of the calcite shells of benthic foraminifera as a potential seawater C-system proxy through a controlled growth experiment with two deep-sea species (*Bulimina marginata* and *Cassidulina laevigata*) and one intertidal species (*Ammonia* T6). To this aim, we used two experimental set-ups to decouple as much as possible the individual components of the carbonate system, i.e., changing pH at constant dissolved inorganic carbon (DIC) and changing DIC at constant pH. Four climatic chambers were used with different controlled concentrations of atmospheric pCO$_2$ (180 ppm, 410 ppm, 1000 ppm, 1500 ppm). Our results demonstrated that pH did not influence the survival and growth of the three species. However, low DIC conditions (879 μmol kg^{-1}) negatively affected *B. marginata* and *C. laevigata* through reduced growth, whereas no effect was observed for *Ammonia* T6. Our results also showed that Sr/Ca was positively correlated with total Alkalinity (TA), DIC and bicarbonate ion concentration ([HCO$_3^-$]) for *Ammonia* T6 and *B. marginata*; i.e., DIC and/or [HCO$_3^-$] were the main controlling factors. For these two species, the regression models were coherent with published data (existing so far only for *Ammonia* T6) and showed overall similar slopes but different intercepts, implying species-specific effects. Furthermore, the Sr/Ca - C-system relationship was not impacted by ontogenetic trends between chamber stages, which is a considerable advantage for paleo-applications. This applied particularly to *Ammonia* T6 that calcified many chambers compared to the two other species. However, no correlation with any of the C-system parameters was observed for Sr/Ca in *C. laevigata*. This might imply either a strong species-specific effect and/or a low tolerance to laboratory conditions leading to a physiological stress, thereby impacting the Sr incorporation into the calcite lattice of *C. laevigata*.

1. Introduction

In Earth's geological history, carbon cycle perturbations have had severe consequences (i.e., warming, acidification, and deoxygenation) and their interactive effects were often coupled with extinctions of major species' groups (e.g., Bijma et al., 2013). Moreover, because the ocean is one of the largest carbon reservoirs, the strength of the production of deep and intermediate waters and their consequent carbon content, is a significant control on atmospheric pCO$_2$ (e.g., Stocker and Schmittner, 1997; Ganopolski and Rahmstorf, 2001; Qin et al., 2022). Therefore, accurate reconstructions of past seawater carbonate chemistry are fundamental for i) understanding carbon cycle-climate interactions and feedbacks, either induced naturally or by anthropogenic carbon emissions (e.g., Hönisch et al., 2012; Bijma et al., 2013; Martínez-Botí et al., 2015), and ii) elucidating critical processes and mechanisms in past ocean thermohaline circulation, which have global climate implications

(e.g., Yu et al., 2008, 2014).

Insights into past marine carbon cycling crucially depend on robust proxies for the seawater carbonate system (C-system), and well-designed experiments permit to deconvolve the co-varying parameters (Zeebe and Wolf-Gladrow, 2001). In the ocean, calcifying micro-organisms, such as foraminifera, incorporate various chemical elements from the seawater during calcification. Elements (El/Ca and isotopic ratios) that have been shown to be linked with the C-system in foraminifera are B/Ca and δ^{11}B (e.g., Hönisch et al., 2009; Yu et al., 2007, 2010; Howes et al., 2017; Levi et al., 2019), Li/Ca and δ^7Li (e.g., Vigier et al., 2015; Roberts et al., 2018), U/Ca (e.g., Raitzsch et al., 2011; Keul et al., 2013), Zn/Ca (e.g., Marchitto et al., 2005; van Dijk et al., 2017b) and Sr/Ca (e.g., Dissard et al., 2010a; Dueñas-Bohórquez et al., 2011b; Diz et al., 2012; Yu et al., 2014; Keul et al., 2017). Still, many of these elemental ratios suffer either from analytical constraints (e.g., limited amount of B and Li in small-sized foraminifera usually used in paleoceanography) and/or a limited understanding of the fundamental mechanisms controlling element incorporation in carbonates (e.g., Kaczmarek et al., 2015).

When studying the impact of the C-system on trace and minor element incorporation, strontium has the advantage to be one of the major elements incorporated into foraminiferal calcite, making it analytically very robust with high accuracy and precision (e.g., Dueñas-Bohórquez et al., 2011a; de Nooijer et al., 2014). Foraminiferal Sr/Ca was first proposed as a temperature proxy, mostly from core-top calibration studies (e.g., Rathbun and De Deckker, 1997; Reichart et al., 2003; Mortyn et al., 2005; Rosenthal et al., 2006). Most of these studies, however, emphasized the possibility that Sr/Ca might reflect other parameters co-varying with temperature such as water depth, pressure, dissolution, and/or carbonate ion concentration [CO_3^{2-}]. More recent controlled growth experiments showed a link with seawater Sr/Ca ratio (Langer et al., 2016) and a strong control of the C-system on foraminiferal Sr/Ca (e.g., Dissard et al., 2010a; Dueñas-Bohórquez et al., 2011b; Yu et al., 2014; Raitzsch et al., 2010; Allen et al., 2016; Keul et al., 2017; van Dijk et al., 2017b; Levi et al., 2019). However, the conclusions of these studies are sometimes contradictory regarding the major C-system parameter controlling Sr incorporation. For instance, while the study of Dissard et al. (2010a) showed that the incorporation of Sr increases with increasing [CO_3^{2-}] (increasing pH), Keul et al. (2017) suggested that DIC or [HCO_3^-] are the main controlling factors. Inconsistencies in interpretations are mainly due to incomparable experimental designs. Indeed, the complexity of the C-system necessitates to experimentally deconvolve the impact of the co-varying C-system parameters (pCO$_2$, bicarbonate ion concentration-[HCO_3^-], carbonate ion concentration-[CO_3^{2-}], pH, total alkalinity-TA, dissolved inorganic carbon-DIC, and calcium carbonate saturation state of seawater-Ω_{cc}). Such designs are very complex to set-up, and therefore, except for Keul et al. (2017) and van Dijk et al. (2017b) (mostly focusing on Zn/Ca), to our knowledge, experimental studies investigating the link between foraminiferal Sr/Ca and the C-system employed classical C-system manipulation, i.e., either DIC (injection of CO$_2$ enriched air or water or NaHCO$_3$/Na$_2$CO$_3$ additions) or TA (changing pCO$_2$ with HCl/NaOH additions) manipulation. In both cases, pH and [CO_3^{2-}] co-vary and cannot be decoupled. Moreover, these studies were conducted on either planktonic, intertidal benthic and/or large tropical foraminifera, which could be impacted differently than deep-sea benthic foraminifera.

In this study, we used a decoupled C-system experimental design (where pH and [CO_3^{2-}] are decoupled), similar to that of Keul et al. (2017) and van Dijk et al. (2017b) to investigate the relationship between Sr/Ca and the C-system in two species *Bulimina marginata* and *Cassidulina laevigata* (also referred to as *Cassidulina carinata;* Murray, 2006). For potential comparison with previous studies and to test reproducibility of the results, we added *Ammonia* molecular type T6 (*Ammonia* T6), recently named *Ammonia confertitesta* (Hayward et al., 2021), the same species used by Keul et al. (2017) and van Dijk et al. (2017b). To improve the stability and the monitoring of the set-up, our experiment was performed for the first time with a new generation of

environmental ecological experiment simulators (Ecolab system; CER-EEP – ECOTRON Île de France) using four climatic chambers with different concentrations of atmospheric pCO$_2$ (180 ppm, 410 ppm, 1000 ppm, 1500 ppm). In addition to the Sr/Ca - C-system relationship, we explored the survival and growth of foraminifera under different pH and DIC conditions and tested the effect of ontogeny between chamber stages on the incorporation of Sr into foraminiferal calcite.

2. Material and methods

2.1. Sampling of seawater and foraminifera for culturing experiments

Two hundred liters of natural seawater were sampled in open waters of the Bay of Biscay (45°18.86 N, 01°43.31 W; salinity = 34.7; DIC ~ 2200 µmol kg^{-1}; TA ~ 2400 µmol kg^{-1}; pH total scale = 7.95) the 29th of November 2019 during the ORHAGO 19 cruise (IFREMER) onboard the *R/V* Côtes De La Manche. In the laboratory, seawater was filtered using 0.45 µm WHATMAN filters membranes and autoclaved (at 121 °C for 20 min) to limit bacterial proliferation. This process did not affect the seawater elemental chemistry since values found after the autoclave process (e.g., Sr$_{sw}$ ~ 82 µmol kg^{-1}) were very similar to values found for Atlantic waters (e.g., Wakaki et al., 2017) and no precipitation was observed. To prevent possible foraminiferal dissolution in the most extreme pCO$_2$ condition (1500 ppm), we increased slightly the alkalinity and DIC of the seawater stock by adding Na$_2$CO$_3$ (200 µmol L^{-1}) to obtain DIC values of ~2350 µmol kg^{-1}, TA of ~2700 µmol kg^{-1} and pH total scale ~8.06. Seawater was stored at 4 °C until the experiments started.

Foraminiferal specimens were harvested alive from their natural environment. *Bulimina marginata* and *Cassidulina laevigata* were collected from the surface sediments of the Gullmar Fjord (58°16.86 N, 11°30.514 E; Sweden) at 30–50 m water depth, using the *R/V* Skagerak on the 14th of January 2020. Although these species were harvested at shallow water depths, their depth range extends to outer continental shelf and slope environments in many areas (e.g., ~200–1500 m water depths; Mackensen and Hald, 1988; Van Marle, 1988; Murray, 1991; Fontanier et al., 2003), making them good candidates for paleoceanographic applications. In the following, we will refer to them as "deep-sea species". The shallow water species *Ammonia* T6 was harvested from the intertidal mudflat of Bourgneuf bay (France) on the 13th of January 2020. Sediments were sieved in the field over 63 µm or 125 µm mesh sieves (using onsite seawater) to remove fine particles and 500 µm to remove macrofauna, all with the aim of concentrating foraminifera.

Once in the laboratory (LPG, Angers, France), the collected sediments were placed in 12 °C incubators for 2–3 weeks in a solution containing calcein (10 mg L^{-1} of calcein stain in Instant Ocean artificial seawater-35 psu) with freeze-dried algae *Chlorella*. This way, specimens that calcified new chambers were labelled with calcein and appeared fluorescent under the epifluorescence microscope. This was used as a criterion to select and isolate only active specimens (i.e., specimens that grew new chambers) to be introduced later in the experiment. Therefore, chambers that calcified afterwards in the controlled experiment would appear non-fluorescent (Supplementary material S1). A total of 1320 adult specimens of labelled *Ammonia* T6, 2176 adult specimens of labelled *B. marginata* and 1176 adult specimens of labelled *C. laevigata* were picked out from the 150–250 µm fraction of the sediment under epifluorescent stereomicroscope. Once harvested, the foraminifera were transported in Falcon vials to the Ecolab facility (CEREEP Ecotron, Ile de France), with calcein solution and a small quantity of in situ <38 µm sediment to reduce stress during transportation.

2.2. Experimental set-up and culturing in the Ecolab facility

The Ecolab is a modular structure that includes three gas-tight environmental chambers and one laboratory room (Supplementary material S2). Each environmental chamber (13 m^3 in volume) can be independently and precisely controlled for different conditions (e.g., air
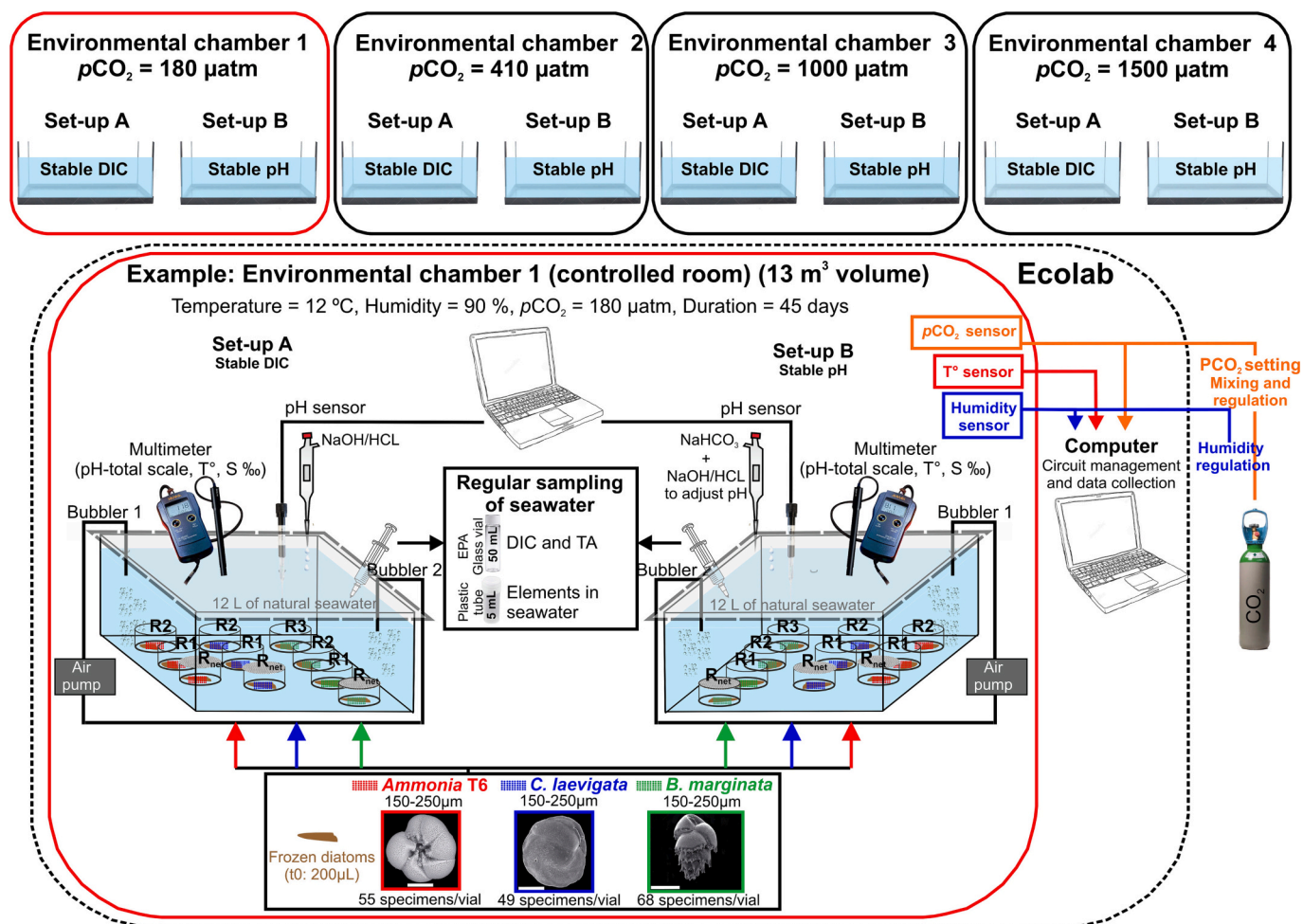
Fig. 1. Schematic of the experimental design. Four climate-controlled chambers with four concentrations of atmospheric pCO$_2$ (180 ppm, 410 ppm, 1000 ppm, 1500 ppm) were used. Temperature and humidity were set respectively at ~12 °C and ~90%. In each chamber, two aquaria corresponding to set-up A (DIC-stable manipulation) and set-up B (pH-stable manipulation) were present. In each aquarium, we put several pseudo-replicates of specimens of the three cultured species. Cf. Material and methods for the details.

temperature, humidity, pCO$_2$, lighting). For this study, we had access to two Ecolabs and used four climate-controlled chambers with four concentrations of atmospheric pCO$_2$ (180 ppm, 410 ppm, 1000 ppm, 1500 ppm). Temperature and humidity were set respectively at ~12 °C and ~90% to limit evaporation. The experimental design is presented in Fig. 1.

Besides precise monitoring and control of air temperature, humidity, pCO$_2$, the large space provided permitted i) manipulation inside each chamber, ii) the use of a large quantity of seawater, iii) culturing a large number of foraminifera and iv) continuous monitoring of pH of the culture media. Indeed, in each climatic chamber, we placed two aquaria (A and B) filled with 12 L of seawater from our initial 200 L stock (no seawater was exchanged between the 12 L and 200 L tanks during the experiment). To ensure homogenization of seawater and equilibration with pCO$_2$, two bubblers were placed in each aquarium. To further limit evaporation, the aquaria were covered by Plexiglas lids. Variability in pH was monitored at 5 min intervals using glass pH electrodes (Consort SP21) continuously immersed in each aquarium. Via an externally connected computer, this continuous measurement allowed early detection of any potential problem in the stability of the system. Absolute pH measurements in total scale were performed using a multimeter (cf. below).ii)

Before adding the foraminiferal specimens, two weeks of pre-test phase were necessary to optimize the geochemistry and the stability of the C-system in the four climatic chambers. During the pre-test phase, and after few days of equilibration with the ambient pCO$_2$ conditions in

each climatic chamber, the carbonate chemistry of seawater was modified chemically following the protocol of Keul et al. (2013, 2017) to decouple as much as possible the co-varying parameters of the C-system (Supplementary material S3; Table 1).

i) Set-up A (DIC-stable manipulation): we added NaOH or HCl to obtain a range of pH and $[CO_3^{2-}]$ while maintaining constant DIC.
ii) Set-up B (pH-stable manipulation): we added NaHCO$_3$ to modify DIC, TA and $[CO_3^{2-}]$, while maintaining a stable pH value.

In the case of the pCO$_2$ condition at 180 ppm (set-up B), the targeted DIC value was below the DIC value of the seawater. Therefore, seawater had to be acidified first with HCl and bubbled with nitrogen to remove excess CO$_2$ from the seawater. Then, the targeted pH and DIC were readjusted with adding NaHCO$_3$. For all treatments, the added volumes of chemicals were estimated using Seacarb package in R software (Gattuso et al., 2019).

After stabilization of seawater chemical parameters during the pre-test phase, foraminifera were put in small glass vials and introduced into the aquaria. Three glass vials (named R$_{net}$, R1, R2) containing each 55 and 49 specimens of *Ammonia* T6 and *C. laevigata* respectively, were put in each aquarium. For *B. marginata*, four glass vials (named R$_{net}$, R1, R2, R3) containing 68 specimens each were put in each aquarium. We covered one of the glass vials (R$_{net}$) with a 100 μm mesh net in case foraminifera were able to climb out of the glass vials. This was to ensure

Table 1

Average values of the C-system parameters, climatic chambers parameters, Sr, Ca and Mg concentrations in seawater, Sr/Ca, Mg/Ca in both seawater and foraminifera and D_{Sr} and D_{Mg} (calculated partition coefficients) for each experimental condition. SD: Standard deviation (1SD). SE: Standard error. SD values of the C-system and seawater parameters are based on the dispersion of datasets (i.e., measurements performed every 1–2 days) relative to the mean in each experimental condition. SE values for El/Ca concentrations in foraminifera represent standard errors of the mean of the dataset (i.e., all final laser ablation measurements; cf. Table 2) in each experimental condition and for each species.

	Set-up A: DIC-stable manipulation				Set-up B: pH-stable manipulation			
	A180	A410	A1000	A1500	B180	B410	B1000	B1500
$p\,CO_2$ (µatm) "nominal"	180	410	1000	1500	180	410	1000	1500
$p\,CO_2$ (µatm) "measured"	180.8	415.9	998.1	1496.3	180.8	415.9	998.1	1496.3
SD $p\,CO_2$ (µatm) "measured"	5.7	19.6	45.5	63.2	5.7	19.6	45.5	63.2
DIC (µmol kg^{-1} SW)	2354.4	2398.2	2372.2	2421.8	879.4	2399.0	4782.1	7131.7
SD DIC (µmol kg^{-1} SW)	36.3	42.6	54.9	26.6	22.1	33.9	38.2	71.2
TA (µmol kg^{-1} SW)	2911.8	2733.9	2558.1	2539.2	1028.8	2719.4	5274.4	7811.8
SD TA (µmol kg^{-1} SW)	15.5	19.3	17.1	28.5	12.6	25.8	17.9	15.0
pH (total scale)	8.40	8.07	7.73	7.56	7.99	8.06	8.02	8.02
SD pH (total scale)	0.04	0.03	0.02	0.02	0.07	0.03	0.01	0.01
$[CO_3^{2-}]$ (µmol kg^{-1} SW)	328.2	169.4	79.7	55.0	52.2	165.6	304.9	457.8
SD $[CO_3^{2-}]$ (µmol kg^{-1} SW)	28.4	12.7	4.9	3.2	8.3	12.3	12.2	18.4
$[HCO_3^-]$ (µmol kg^{-1} SW)	2018.5	2210.9	2253.0	2306.9	819.3	2215.1	4437.2	6614.6
SD $[HCO_3^-]$ (µmol kg^{-1} SW)	41.4	40.8	52.2	25.4	21.7	33.1	37.2	68.2
Omega calcite (Ω_{cc})	7.8	4.0	1.9	1.3	1.2	3.9	7.2	10.9
SD Omega calcite (Ωcc)	0.8	0.4	0.1	0.1	0.2	0.3	0.4	0.7
Temperature climatic chamber (°C)	12.1	11.7	12.1	12.2	12.1	11.7	12.1	12.2
SD Temperature climatic chamber (°C)	0.4	0.7	0.34	0.12	0.4	0.7	0.34	0.12
Humidity climatic chamber (%)	88.1	84.6	81.9	89.3	88.1	84.6	81.9	89.3
SD Humidity climatic chamber (%)	6.4	5.3	12.0	1.2	6.4	5.3	12.0	1.2
Temperature aquaria (°C)	11.5	11.4	11.6	11.7	11.6	11.3	11.5	11.8
SD Temperature aquaria (°C)	0.22	0.27	0.17	0.05	0.19	0.25	0.13	0.05
Salinity	34.9	35.4	35.5	35.2	35.0	35.5	35.5	35.3
SD Salinity	0.12	0.27	0.07	0.12	0.15	0.09	0.07	0.09
Sr_{sw} (µmol kg^{-1})	81.77	82.38	82.27	82.77	82.15	81.90	83.13	81.90
SD Sr_{sw} (µmol kg^{-1})	0.55	1.07	0.57	0.61	0.64	0.52	0.65	0.63
Mg_{sw} (mmol kg^{-1})	51.81	52.79	52.82	52.43	51.89	52.70	52.60	51.79
SD Mg_{sw} (mmol kg^{-1})	0.47	0.44	0.40	0.35	0.64	0.40	0.25	0.26
Ca_{sw} (mmol kg^{-1})	9.89	9.99	9.94	10.03	9.98	9.86	10.09	9.88
SD Ca_{sw} (mmol kg^{-1})	0.04	0.12	0.05	0.05	0.06	0.05	0.05	0.05
Sr/Ca_{sw} (mmol mol^{-1})	8.27	8.25	8.27	8.25	8.23	8.31	8.24	8.29
SD Sr/Ca_{sw} (mmol mol^{-1})	0.05	0.05	0.04	0.06	0.06	0.07	0.07	0.06
Sr/Ca *Ammonia* T6 (mmol mol^{-1})	1.51	1.45	1.37	1.35	1.16	1.41	1.53	1.72
SE Sr/Ca *Ammonia* T6 (mmol mol^{-1})	0.02	0.03	0.02	0.02	0.01	0.02	0.02	0.03
D_{Sr} *Ammonia* T6	0.18	0.18	0.17	0.16	0.14	0.17	0.19	0.21
Sr/Ca *B. marginata* (mmol mol^{-1})	1.30	1.27	1.28	1.24	1.16	1.22	1.44	1.52
SE Sr/Ca *B. marginata* (mmol mol^{-1})	0.02	0.02	0.02	0.02	0.06	0.01	0.02	0.02
D_{Sr} *B. marginata*	0.16	0.15	0.15	0.15	0.14	0.15	0.17	0.18
Sr/Ca *C. laevigata* (mmol mol^{-1})	1.18	1.10	1.11	1.09	1.22	1.13	1.25	1.20
SE Sr/Ca *C. laevigata* (mmol mol^{-1})	0.03	0.02	0.03	0.02	0.02	0.02	0.02	0.04
D_{Sr} *C. laevigata*	0.14	0.13	0.13	0.13	0.15	0.14	0.15	0.15
Mg/Ca_{sw} (mmol mol^{-1})	5238.7	5285.2	5312.2	5226.7	5199.5	5346.4	5212.4	5240.0
SD Mg/Ca_{sw} (mmol mol^{-1})	39.6	56.2	42.5	47.1	42.3	42.1	24.3	31.0
Mg/Ca *Ammonia* T6 (mmol mol^{-1})	1.12	1.30	1.10	1.17	1.44	1.02	0.92	1.05
SE Mg/Ca *Ammonia* T6 (mmol mol^{-1})	0.14	0.20	0.10	0.12	0.08	0.09	0.07	0.10
D_{Mg} *Ammonia* T6	$2.13\,10^{-4}$	$2.45\,10^{-4}$	$2.08\,10^{-4}$	$2.24\,10^{-4}$	$2.76\,10^{-4}$	$1.91\,10^{-4}$	$1.76\,10^{-4}$	$2.01\,10^{-4}$
Mg/Ca *B. marginata* (mmol mol^{-1})	2.87	2.60	2.45	2.91	2.44	2.44	2.22	1.69
SE Mg/Ca *B. marginata* (mmol mol^{-1})	0.34	0.42	0.27	0.59	0.48	0.14	0.32	0.13
D_{Mg} *B. marginata*	$5.47\,10^{-4}$	$4.92\,10^{-4}$	$4.61\,10^{-4}$	$5.57\,10^{-4}$	$4.69\,10^{-4}$	$4.56\,10^{-4}$	$4.25\,10^{-4}$	$3.23\,10^{-4}$
Mg/Ca *C. laevigata* (mmol mol^{-1})	1.96	2.32	2.30	1.81	2.18	2.53	2.33	2.67
SE Mg/Ca *C. laevigata* (mmol mol^{-1})	0.38	0.24	0.15	0.25	0.25	0.24	0.16	0.56
D_{Mg} *C. laevigata*	$3.75\,10^{-4}$	$4.38\,10^{-4}$	$4.33\,10^{-4}$	$3.47\,10^{-4}$	$4.19\,10^{-4}$	$4.72\,10^{-4}$	$4.48\,10^{-4}$	$5.10\,10^{-4}$

that in at least one of the glass vials, we could recover all specimens easily at the end of the experiment. All glass vials were not covered in case the net creates a microenvironment in which the seawater is not totally in equilibrium with the ambient water of the aquarium. Because R_{net}, R1, R2, R3 are put together in the same aquarium, they are not true replicates and will be referred to hereafter as pseudo-replicates. The culturing experiment lasted ~45 days, during which the foraminifera were fed three times with 200 μL of frozen cells of the algae *Phaeo-dactylum tricurnutum*, diluted in seawater.

In the aquaria, pH, TA, DIC, salinity, and temperature of the seawater were measured daily or once every two days. For pH, salinity, and temperature, we used a multimeter WTW 3620 ID equipped with a Tetracon sensor for conductivity (and associated temperature) and a SENTIX sensor for pH (and associated temperature). Parallel measurements of seawater pH buffers (Tris purchased from the Certified Reference Materials Laboratory of SCRIPPS and AMP prepared according to the recipe of Dickson et al. (2007)) allowed conversion of the measured potential difference values to pH values on the total scale. For DIC and TA measurements, we sampled ~45 mL of seawater in each aquarium using a 50 mL syringe. The sampled seawater was placed in borosilicate vials with PTFE/silicone septa, that we overfilled to avoid air bubbles, and closed inside the climatic chambers under the correspondent pCO$_2$ conditions. Then, DIC was measured directly after sampling with a Shimadzu TOC-L analyzer. After DIC measurement, the seawater was analyzed for TA by automated titration with a Titrino 785 (Methrom) with certified 0.1 mol kg^{-1} HCl (and 0.6 mol kg^{-1} NaCl) as titrant (Dickson). The accuracy of DIC and TA analyses was verified with a reference seawater standard (Dickson batch 182). The precision of individual samples, reference seawater standard (Dickson batch 182) and in-house seawater standards assessed by three injections for DIC and by three replicate analyses per measurement for TA, was 0.6% and 0.2%, respectively. In our experiment, we used pH total scale, DIC, water temperature and salinity values to calculate C-system parameters using CO$_2$ SYS program (Lewis and Wallace, 1998) with equilibrium constants of Lueker et al. (2000). Because only two C-system parameters are needed as inputs for the CO$_2$ SYS program, TA measurements were only used as an additional control for the outputs of the CO$_2$ SYS program.

For the elemental composition of seawater (Sr, Mg, Ca…), we sampled 5 mL of seawater using a syringe equipped with a cellulose acetate filter (0.2 μm). The filtered water samples were placed in plastic tubes, acidified with concentrated ultrapure nitric acid (HNO$_3$), and stored at 4 °C for later analyses.

At the end of the experiment, each glass vial containing foraminifera was filtered through a 38 μm sieve with natural seawater. Specimens from each vial were transferred to a falcon tube and fixed with ethanol (96%). All vials and sieves were checked under stereomicroscope for the presence of attached specimens.

2.3. Foraminiferal and seawater elements/Ca analyses

In the laboratory, all specimens were checked under epifluorescent microscope to assess their survival (i.e., the percentage of specimens with a full yellow/orange cytoplasm) and growth (i.e., the percentage of specimens that calcified new chambers) at the end of the experiment. Specimens that calcified one or more chambers during the experiments were cleaned with 5% NaOCl (~1 h incubation) to remove organic material. Specimens were rinsed before and after with ultra-pure water. The newly formed chambers were analyzed for elemental concentrations using laser ablation–inductively coupled plasma–mass spectrometry (LA-ICP-MS).

For *Ammonia* T6, measurements were performed at LPG (Nantes, France) using an Excimer laser Analyte.G2 (Photon Machine) at a wavelength of 193 nm, coupled with a quadrupole ICP-MS (Varian). The ablation was conducted in a helium atmosphere. Pulse repetition rate was set at 5 Hz, with a fluence of 0.91 J cm^{-2} (10% of the laser energy output). Depending on the size of the analyzed chamber, ablation spots were 50 or 65 μm in diameter. ^{43}Ca isotope was used as an internal

standard, and the SRM NIST 610 glass standard (National Institute of Science and Technology, USA) (Jochum et al., 2011) was used for the calibration of minor and trace elements. The NIST standard was measured every 10–15 samples with a fluence of 0.91 J cm^{-2}, a repetition rate of 5 Hz and ablation spots of 85 μm (cf. supplementary material S4a for the total operating parameters). The abundance of the following isotopes was measured: ^{24}Mg, ^{25}Mg, ^{27}Al, ^{43}Ca, ^{44}Ca, ^{66}Zn, ^{88}Sr, and ^{138}Ba and used to calculate elemental concentrations using average cosmic isotope ratios. The quality of trace elemental analyses of the foraminiferal calcite was further checked using the matrix-matched calcite standard MACS-3 (MicroAnalytical Carbonate Standard, United States Geological Survey, 2012), and one NIOZ foraminifera in-house standard, NFHS, measured every 10–15 samples. Standardization was performed by bracketing analyses of SRM NIST 610 associated with each block of 10–15 samples. Raw counts were converted to element concentrations using the Glitter data reduction software developed by the GEMOC ARC National Key Centre and CSIRO and assuming 56 wt% CaO in CaCO$_3$. Repeatability, expressed as the relative standard deviation (RSD), of all MACS-3 analyses (average of the four sessions; 44 data points), was 3% for ^{25}Mg/Ca, 6% for Zn/Ca, 3% for Sr/Ca, and 3% Ba/Ca, and accuracies were 99%, 128%, 104%, and 105% respectively (Supplementary material S4b; c).

The newly formed chambers of *B. marginata* and *C. laevigata* were ablated and measured at NIOZ using LA-ICP-MS. The system used consists of a NWR193UC (Elemental Scientific Lasers) with an ArF Excimer laser (Coherent Excistar XS) with deep UV (193 nm wavelength) coupled with a quadrupole ICP-MS (iCAP-Q, Thermo Fisher Scientific). Single chambers of *B. marginata* were ablated with a laser energy of 1 J cm^{-2}, a repetition rate of 6 Hz, and an ablation spot size of 40 μm in diameter, whereas single chambers of *C. laevigata* were ablated with a laser energy of 0.5 J cm^{-2}, a repetition rate of 4 Hz, and a spot size of 40 μm (cf. supplementary material S4a for the total operating parameters). At the start of each series, SRM NIST 610 calibration and quality control reference material carbonate standards were analyzed, including JCt-1 (giant clam), JCp-1 (coral, *Porites* sp.; Okai et al., 2002), MACS-3 (synthetic calcium carbonate) and a foraminifera standard NFHS-2-NP (Boer et al., 2022). Carbonate standards were ablated with the same laser settings as used for the foraminifera. SRM NIST 610 was ablated using an energy of 4 J cm^{-2}. SRM NIST 610 was preferred over MACS-3 for calibration, because MACS-3 was found to be too inhomogeneous at a spot size of 40 μm. NFHS-2-NP standard was used to monitor drift after every fourth sample. NFHS-2-NP is the preferred homogeneous reference material for drift monitoring at NIOZ as it shows lower gas blanks for some elements than SRM NIST 610 (e.g., Na). The calibrated data of NFHS-2-NP using SRM NIST 610 without drift correction were used to calculate drift correction factors. The first four NFHS-2-NP standards directly measured after the calibration standards were assumed to undergo no drift. Although instrumental drift was small, drift corrections were made to improve the accuracy. The isotopes of ^{24}Mg, ^{25}Mg, ^{43}Ca, ^{66}Zn, and ^{88}Sr were measured for *B. marginata* and ^{25}Mg, ^{43}Ca, ^{66}Zn, and ^{88}Sr for *C. laevigata* using ^{43}Ca as an internal standard. Backgrounds were measured for 60 s and the number of shots was 120. Raw counts were converted to element concentrations using an adapted version of the MATLAB based program Signal Integration for Laboratory Laser Systems (Guillong et al., 2008). This modification allows to import Thermo Qtegra software sample list and ICP-MS data files, screen shots, and laser LOG files (as described in Mezger et al., 2016 and van Dijk et al., 2017a). The region of interest of the signal is automatically set by the Matlab scripts and fine-tuned manually using the intensity signals and screen shots of the ablation foraminifera (made automatically every 1.5 s). Repeatability, expressed as the relative standard deviation (RSD), of all NFHS-2-NP analyses (average of the five sessions; 325 data points), was 2% for ^{25}Mg/Ca, 11% for Zn/Ca, and 2% for Sr/Ca, and accuracies were 94%, 99%, and 102% respectively (Supplementary material S4b; c).

For the three species, integration profiles were manually selected, by discarding the initial part of the signals showing Al and/or Mg peaks,

which can be used as a sign of contamination, and by monitoring the decrease in Ca counts. In total, 436 ablation measurements were performed on chambers of *Ammonia* T6 that calcified under experimental conditions, 285 on *B. marginata* and 288 on *C. laevigata*. In all, 13%, 17% and 46% of these profiles, for *Ammonia* T6, *B. marginata*, and *C. laevigata* respectively, were not included in the final analyses (cf. raw data https://doi.org/10.17882/89623) because they were either too short or because there was doubt on the fluorescence of the newly formed chambers, especially for *C. laevigata*. As such, and for each condition, between 6 and 57 measurements were obtained for each species (Table 2). When several chambers were calcified under controlled conditions, it was possible to perform LA-ICP-MS measurements on successively added chambers, from chamber n (latest calcified chamber) to older ones (n-1, n-2…). This allowed evaluating a potential ontogenetic effect.

Measurements of the elemental composition of seawater (Sr, Mg, Ca…) were performed by an ICP-OES ICAP 6300 Thermo-Fischer in LPG (Nantes) (Table 1). Samples were diluted 1:50 with 1% HNO$_3$. Calibration was performed with seven multi-element standards, covering the concentration range of the samples, prepared by properly diluting single-element stock solutions (1000 µg g^{-1}). All standards and the blank were measured at the beginning, midpoint, and end of the analytical run; three replicate readings were performed on standards, blank and samples.

The partitioning coefficients of strontium (D$_{Sr}$) and magnesium (D$_{Mg}$) were calculated following the equations: D$_{El}$ = (El/Ca)$_{calcite}$/(El/Ca)$_{seawater}$ (Table 1).

Scanning Electron Microscope (SEM) pictures (Supplementary material S5) were obtained at LPG (Angers, France) using a Tabletop Microscope Hitachi TM4000Plus.

Table 2

Number of LA-ICP-MS Sr/Ca measurements per species, condition and replicate. "Initial" refers to the total performed measurements. "Final" refers to the measurements selected after discarding the profiles with very short counting time (chambers that broke rapidly), with high contamination, and doubtful chambers in terms of calcification (cf. 1n? in Fig. 3). "Not available" refers to the absence of the replicate, and "Not measured" refers to the fact that the measurements were not performed.

	Number of LA-ICP-MS measurements									
	R$_{net}$		R1		R2		R3		Total	
	Initial	Final	Initial	Final	Initial	Final	Initial	Final	Initial	Final
Ammonia T6										
A180	26	23	10	8	10	8			46	**39**
A410	31	24	8	8	13	10			52	**42**
A1000	30	29	10	4	15	12			55	**45**
A1500	27	27	10	9	0	0	Not available		37	**36**
B180	29	24	10	6	28	25			67	**55**
B410	21	18	12	12	24	23			57	**53**
B1000	27	26	9	7	23	20			59	**53**
B1500	31	29	11	10	12	8			54	**47**
B. marginata										
A180	40	27			13	13			53	**40**
A410	17	14			7	7			24	**21**
A1000	19	18			7	7			26	**25**
A1500	33	21	Not measured		6	2	Not measured		39	**23**
B180	2	2			4	4			6	**6**
B410	51	36			8	8			59	**44**
B1000	29	28			17	16			46	**44**
B1500	22	22			10	10			32	**32**
C. laevigata										
A180	9	0	3	0	16	7			28	**7**
A410	10	5	13	5	12	6			35	**16**
A1000	14	9	5	3	14	1			33	**13**
A1500	11	7	22	4	11	10	Not available		44	**21**
B180	0	0	6	0	11	6			17	**6**
B410	27	21	4	4	13	4			44	**29**
B1000	29	16	14	7	14	2			57	**25**
B1500	13	8	13	4	4	4			30	**16**

2.4. Statistical analyses

To compare survival and growth and El/Ca ratios (individual chamber analyses) between the treatments and the pseudo-replicates (Figs. 2; 5 and 6), we tested first the data for normality (Shapiro-Wilk's test). Because a normal distribution was not observed for all data sets, we performed pairwise comparison with Kruskal Wallis (i.e., a non-parametric test that does not assume a normal distribution of the underlying data). These tests were performed using Past software (Hammer et al., 2001). Dixon's test (Dixon, 1950, 1951) was performed to identify outliers in the growth percentages between experimental conditions presented in Fig. 3. Linear regression analyses between foraminiferal El/Ca (individual chamber analyses) and the C-system parameters were performed using the statistics environment R (R Development Core Team, 2012; http://www.R-project.org) (Table 3). To test the differences between regression models, we performed a one-way ANCOVA using Past software (Hammer et al., 2001) (Table 4). Spearman's (non-parametric) rank-order correlation coefficient (Spearman, 1904) was calculated using Past software (Hammer et al., 2001) to assess the presence/absence of ontogenetic trends in foraminiferal El/Ca (individual chamber analyses) according to the position of the newly formed chambers (Table 5). A p-value of 0.05 was considered as significant for all statistical tests.

3. Results

3.1. Stability of the experimental set-up

In each environmental chamber, the measured pCO$_2$ was similar to the nominal pCO$_2$ ($<$1.5% difference) and showed stable values over the experimental period with a relative standard deviation (RSD) of $<$5% (Table 1). Air temperature was stable in each environmental chamber with a RSD of $\leq$6% and ranged between chambers from an average of 11.7 $\pm$ 0.7 to 12.2 $\pm$ 0.12 °C (Table 1). In each aquarium, temperature and salinity values were stable with a RSD of $<$2.5% (Table 1). Between the eight aquaria, the culture media temperatures and salinities varied from an average of 11.3 $\pm$ 0.2 to 11.8 $\pm$ 0.1 °C and 34.9 $\pm$ 0.1 to 35.5 $\pm$ 0.1 respectively (Table 1). The measured C-system parameters (DIC, TA and pH total scale) were stable in each of the eight conditions with a $<$ 5% RSD (Table 1; Supplementary material S3). For set-up A, DIC was stable at an average of 2387 $\pm$ 48 µmol kg^{-1}, TA and the calculated [HCO$_3^-$] slightly varied between 2539 $\pm$ 28 and 2912 $\pm$ 15 µmol kg^{-1} and between 2018 $\pm$ 41 and 2306 $\pm$ 25 µmol kg^{-1} respectively and a wide range was obtained for pH total scale (7.56 $\pm$ 0.02 – 8.40 $\pm$ 0.04), the calculated [CO$_3^{2-}$] (55 $\pm$ 3 – 328 $\pm$ 29 µmol kg^{-1}) and the calculated Ω_{cc} (1.3 $\pm$ 0.1 – 7.8 $\pm$ 0.8). For set-up B, pH total scale was constant at an average of 8.02 $\pm$ 0.04 while a wide range was obtained for DIC (879 $\pm$ 22 – 7131 $\pm$ 71 µmol kg^{-1}), TA (1029 $\pm$ 13 – 7812 $\pm$ 15 µmol kg^{-1}), [HCO$_3^-$] (819 $\pm$ 30 – 6615 $\pm$ 68 µmol kg^{-1}), [CO$_3^{2-}$] (52 $\pm$ 8 – 457 $\pm$ 18 µmol kg^{-1}), and Ω_{cc} (1.2 $\pm$ 0.2 – 10.9 $\pm$ 0.7) (Table 1). Sr$_{sw}$, Mg$_{sw}$, Ca$_{sw}$, Sr/Ca$_{sw}$ and Mg/Ca$_{sw}$ values were stable in each aquarium and similar between the eight aquaria (81.8 $\pm$ 0.5 – 83.1 $\pm$ 0.6 µmol kg^{-1}, 51.8 $\pm$ 0.3 – 52.8 $\pm$ 0.4 mmol kg^{-1}, 9.9 $\pm$ 0.05 – 10.1 $\pm$ 0.05 mmol kg^{-1}, 8.23 – 8.31 mmol mol^{-1} and 5199 – 5346 mmol mol^{-1} respectively) (Table 1).

3.2. Survival and growth

Many specimens of the three species survived and grew new chambers in all experimental conditions (Fig. 2a). Nevertheless, lower survival and growth percentages on average were found for *B. marginata* (55 $\pm$ 10% and 20 $\pm$ 15%, respectively) and *C. laevigata* (66 $\pm$ 19% and 16 $\pm$ 15%, respectively) compared to *Ammonia* T6 (87 $\pm$ 16% and 84 $\pm$ 11%, respectively) (Fig. 2a). When considering the eight experimental conditions together, there was no significant difference between the pseudo-replicates in terms of survival and growth, except for R1 where *Ammonia* T6 recorded the lowest values (Fig. 2b; c). Survival

percentages were similar in the eight conditions for the three species. While the growth percentages of *Ammonia* T6 were similar in the different conditions (> 80%, except at condition A180 recording values of ~79%), the lowest growth percentages were recorded in the low DIC condition B180, for both *B. marginata* and *C. laevigata* (Fig. 3). These

observations were confirmed statistically by the Dixon's test identifying the A180 growth value of *Ammonia* T6 and the B180 growth values of the too deep-sea species as outliers. Although survival and growth rates of the three species in R$_{net}$ were not significantly different from the other pseudo-replicates when considering the eight conditions together (Fig. 2), we observed that no specimens of *C. laevigata* survived and calcified new chambers in the R$_{net}$ of the low DIC condition B180. In the same condition (B180) and pseudo-replicate (R$_{net}$), the survival rate of *B. marginata* was not significantly different from the other conditions and pseudo-replicates (69%), but the lowest growth (1.6%) was found compared to the other pseudo-replicates of B180 (~ 12%). For *Ammonia* T6, the net had no effect on its survival and growth in the B180 condition. In terms of shell aspect however, the three species showed high degrees of dissolution in the B180-R$_{net}$ condition whereas no consistent dissolution patterns were found in the other replicates and conditions
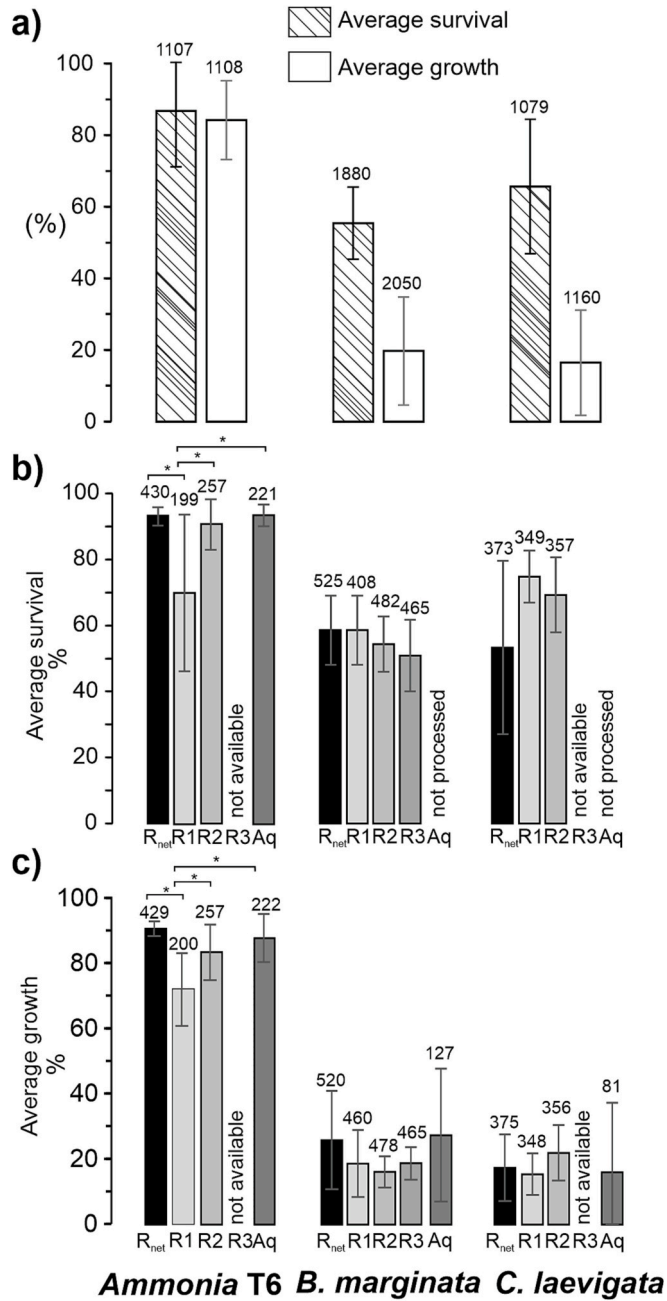

Fig. 2. Survival and growth. (a) Average survival (i.e., average percentages of specimens with full cytoplasm) and growth (i.e., average percentages of specimens that calcified *i* new chambers) for each species, all replicates and conditions combined. (b; c) Average survival and growth for each species and each replicate, all conditions combined. R$_{net}$, R1, R2 and R3 are the used pseudo-replicates (Fig. 1). Aq corresponds to specimens found at the end of the experiment outside of the glass vials in the aquarium seawater. The number of data points (i.e., specimens) is indicated on top of the histograms. The slight difference in the number of data points (indicated on top of the histograms) between survival and growth data is due to the loss of some specimens between the two manipulations. The absence of data is either due to the initial absence of the replicate or the non-processing of the data. The pairwise significant differences ($p < 0.05$) are indicated with a bracket and an asterisk (Kruskal Wallis test).
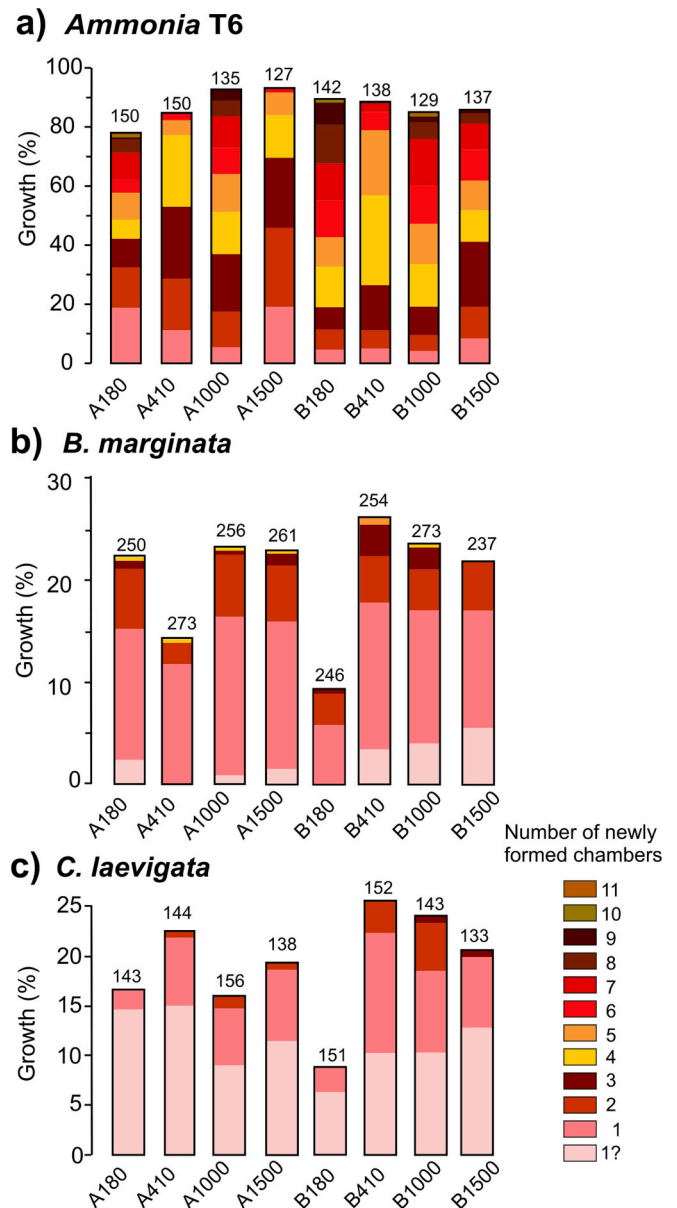
Fig. 3. Total percentages of specimens that calcified 1 to 11 new chambers in each condition for *Ammonia* T6, *B. marginata* and *C. laevigata* respectively, all replicates combined. Growth refers to the percentages of specimens that calcified *i* new chambers. "1?" indicates a doubt in the determination of the newly calcified chamber. Be aware of the different scaling between the graphs. The number of data points is indicated on top of the histograms.

Table 3

Linear regression analyses between foraminiferal Sr/Ca and the respective C-system parameters. Listed are the intercepts with the y-axis and the slope together with the associated standard errors (SE) for these parameters, and the *p*-values, and R^2 of the regression analyses.

		All treatments combined						Set-up A: DIC-stable manipulation						Set-up B: pH-stable manipulation					
		Intercep	SE	Slope	SE	p	R^2	Intercept	SE	Slope	SE	p	R^2	Intercept	SE	Slope	SE	p	R^2
Ammonia T6	pCO_2 (µatm) "measured"	1.30	0.02	$1.75\ 10^{-4}$	$1.97\ 10^{-5}$	$< 2.2\ 10^{-16}$	0.18	1.52	0.02	$-1.22\ 10^{-4}$	$1.79\ 10^{-5}$	$1.86\ 10^{-10}$	0.22	1.14	0.02	$4.09\ 10^{-4}$	$2.05\ 10^{-5}$	$< 2.2\ 10^{-16}$	0.66
	DIC (µmol kg^{-1} SW)	1.19	0.01	$8.11\ 10^{-5}$	$4.07\ 10^{-6}$	$< 2.2\ 10^{-16}$	0.52	4.69	4.69	$-1.37\ 10^{-3}$	$3.91\ 10^{-4}$	$6.04\ 10^{-4}$	0.07	1.12	0.02	$8.95\ 10^{-5}$	$4.28\ 10^{-6}$	$< 2.2\ 10^{-16}$	0.69
	TA (µmol kg^{-1} SW)	1.17	0.01	$7.60\ 10^{-5}$	$3.69\ 10^{-6}$	$< 2.2\ 10^{-16}$	0.54	0.33	0.16	$4.09\ 10^{-4}$	$5.89\ 10^{-5}$	$9.56\ 10^{-11}$	0.23	1.11	0.02	$8.28\ 10^{-5}$	$3.94\ 10^{-6}$	$< 2.2\ 10^{-16}$	0.69
	pH (total scale)	-0.27	0.39	$2.13\ 10^{-1}$	$4.90\ 10^{-2}$	$1.45\ 10^{-5}$	0.05	-0.12	0.22	$1.95\ 10^{-1}$	$2.78\ 10^{-2}$	$7.10\ 10^{-11}$	0.24	-21.71	5.30	2.89	0.66	$2.02\ 10^{-5}$	0.09
	[CO_3^{2-}] (µmol kg^{-1} SW)	1.22	0.01	$1.10\ 10^{-3}$	$5.46\ 10^{-5}$	$< 2.2\ 10^{-16}$	0.53	1.34	0.02	$5.54\ 10^{-4}$	$8.35\ 10^{-5}$	$5.06\ 10^{-10}$	0.22	1.11	0.02	$1.42\ 10^{-3}$	$6.59\ 10^{-5}$	$< 2.2\ 10^{-16}$	0.70
	[HCO_3^-] (µmol kg^{-1} SW)	1.19	0.01	$8.62\ 10^{-5}$	$4.44\ 10^{-6}$	$< 2.2\ 10^{-16}$	0.51	2.56	0.18	$-5.16\ 10^{-4}$	$8.41\ 10^{-5}$	$6.81\ 10^{-9}$	0.19	1.12	0.02	$9.64\ 10^{-5}$	$4.61\ 10^{-6}$	$< 2.2\ 10^{-16}$	0.69
	Omega calcite (Ω_{cc})	1.21	0.01	$4.60\ 10^{-2}$	$2.30\ 10^{-3}$	$< 2.2\ 10^{-16}$	0.53	1.34	0.02	$2.32\ 10^{-2}$	$3.50\ 10^{-3}$	$5.22\ 10^{-10}$	0.22	1.11	0.02	$5.96\ 10^{-2}$	$2.77\ 10^{-3}$	$< 2.2\ 10^{-16}$	0.70
B. marginata	pCO_2 (µatm) "measured"	1.21	0.02	$1.15\ 10^{-4}$	$1.68\ 10^{-5}$	$5.13\ 10^{-11}$	0.15	1.27	0.01	$-2.46\ 10^{-5}$	$1.49\ 10^{-5}$	0.10	0.02	1.09	0.02	$3.14\ 10^{-4}$	$2.12\ 10^{-5}$	$< 2.2\ 10^{-16}$	0.62
	DIC (µmol kg^{-1} SW)	1.08	0.01	$6.71\ 10^{-5}$	$3.87\ 10^{-6}$	$< 2.2\ 10^{-16}$	0.52	2.85	0.70	$-6.70\ 10^{-4}$	$2.92\ 10^{-4}$	0.02	0.04	1.06	0.02	$7.05\ 10^{-5}$	$4.87\ 10^{-6}$	$< 2.2\ 10^{-16}$	0.61
	TA (µmol kg^{-1} SW)	1.07	0.01	$6.25\ 10^{-5}$	$3.57\ 10^{-6}$	$< 2.2\ 10^{-16}$	0.53	1.06	0.14	$6.90\ 10^{-5}$	$4.99\ 10^{-5}$	0.17	0.01	1.05	0.02	$6.54\ 10^{-5}$	$4.52\ 10^{-6}$	$< 2.2\ 10^{-16}$	0.61
	pH (total scale)	1.00	0.29	$3.78\ 10^{-2}$	$3.59\ 10^{-2}$	0.29	0.00	0.96	0.18	$3.62\ 10^{-2}$	$2.32\ 10^{-2}$	0.12	0.02	36.09	4.78	-4.32	0.59	$2.58\ 10^{-11}$	0.28
	[CO_3^{2-}] (µmol kg^{-1} SW)	1.15	0.01	$6.80\ 10^{-4}$	$5.80\ 10^{-5}$	$< 2.2\ 10^{-16}$	0.33	1.23	0.01	$1.02\ 10^{-4}$	$6.85\ 10^{-5}$	0.14	0.02	1.05	0.02	$1.13\ 10^{-3}$	$8.01\ 10^{-5}$	$< 2.2\ 10^{-16}$	0.60
	[HCO_3^-] (µmol kg^{-1} SW)	1.09	0.01	$7.13\ 10^{-5}$	$4.16\ 10^{-6}$	$< 2.2\ 10^{-16}$	0.52	1.49	0.14	$-1.10\ 10^{-4}$	$6.63\ 10^{-5}$	0.10	0.02	1.06	0.02	$7.59\ 10^{-5}$	$5.23\ 10^{-6}$	$< 2.2\ 10^{-16}$	0.61
	Omega calcite (Ω_{cc})	1.15	0.01	$2.85\ 10^{-2}$	$2.44\ 10^{-3}$	$< 2.2\ 10^{-16}$	0.33	1.23	0.01	$4.26\ 10^{-3}$	$2.87\ 10^{-3}$	0.14	0.02	1.05	0.02	$4.77\ 10^{-2}$	$3.37\ 10^{-3}$	$< 2.2\ 10^{-16}$	0.60
C. laevigata	pCO_2 (µatm) "measured"	1.16	0.02	$2.10\ 10^{-5}$	$1.92\ 10^{-5}$	0.277	0.01	1.16	0.02	$-1.07\ 10^{-5}$	$2.14\ 10^{-5}$	0.62	0.005	1.14	1.14	$6.08\ 10^{-5}$	$2.98\ 10^{-5}$	0.05	0.05
	DIC (µmol kg^{-1} SW)	1.13	0.02	$1.49\ 10^{-5}$	$5.22\ 10^{-6}$	0.005	0.06	0.68	1.09	$-1.97\ 10^{-54}$	$4.53\ 10^{-4}$	0.67	0.003	1.14	0.03	$1.23\ 10^{-5}$	$6.72\ 10^{-6}$	0.07	0.04
	TA (µmol kg^{-1} SW)	1.12	0.02	$1.38\ 10^{-5}$	$4.79\ 10^{-6}$	0.005	0.06	0.92	0.22	$8.76\ 10^{-5}$	$8.41\ 10^{-5}$	0.30	0.019	1.14	0.03	$1.13\ 10^{-5}$	$6.23\ 10^{-6}$	0.07	0.04
	pH (total scale)	0.78	0.34	$4.98\ 10^{-2}$	$4.34\ 10^{-2}$	0.253	0.01	0.92	0.29	$2.95\ 10^{-2}$	$3.75\ 10^{-2}$	0.44	0.011	16.30	4.54	-1.88	0.57	0.001	0.13
	[CO_3^{2-}] (µmol kg^{-1} SW)	1.14	0.02	$1.97\ 10^{-4}$	$6.92\ 10^{-5}$	0.005	0.06	1.14	0.02	$1.18\ 10^{-4}$	$1.22\ 10^{-4}$	0.34	0.017	1.14	0.03	$1.81\ 10^{-4}$	$1.09\ 10^{-4}$	0.10	0.04
	[HCO_3^-] (µmol kg^{-1} SW)	1.13	0.02	$1.60\ 10^{-5}$	$5.62\ 10^{-6}$	0.005	0.06	1.35	0.27	$-8.95\ 10^{-5}$	$1.22\ 10^{-4}$	0.47	0.010	1.14	0.03	$1.33\ 10^{-5}$	$7.23\ 10^{-6}$	0.07	0.04
	Omega calcite (Ω_{cc})	1.14	0.02	$8.28\ 10^{-3}$	$2.91\ 10^{-3}$	0.005	0.06	1.14	0.02	$4.94\ 10^{-3}$	$5.11\ 10^{-3}$	0.34	0.017	1.14	0.03	$7.64\ 10^{-3}$	$4.57\ 10^{-3}$	0.10	0.04

Table 4

Results of ANCOVA test analyses between foraminiferal Sr/Ca and [HCO$_3^-$] comparing *Ammonia* T6 (this study) and *Ammonia* T6 (Keul et al., 2017) regression models and *Ammonia* T6 and *B. marginata* (this study) regression models.

Ammonia T6 (this study) vs *Ammonia* T6 (Keul et al., 2017)		Sum of squares	df	Mean square	F	p (same)
	Adjusted mean	0.06	1	0.06	2.1	0.15
	Adjusted error	16.9	636	0.03		
	Adjusted total	17.0	637			
	Homogeneity (equality) of slopes					
	F	40.4				
	p (same)	3.9 10^{-10}				
Ammonia T6 (this study) vs *B. marginata* (this study)		Sum of squares	df	Mean square	F	p (same)
	Adjusted mean	3.33	1	3.33	200.7	8.73 10^{-40}
	Adjusted error	10.5	635	0.02		
	Adjusted total	13.9	636			
	Homogeneity (equality) of slopes					
	F	5.4				
	p (same)	0.02				

Table 5

Spearman's (non-parametric) rank-order correlation coefficients (r) and the p-values between foraminiferal El/Ca (individual chamber analyses) and the position of the newly formed chambers (from the oldest to the latest formed), all treatments combined.

	Ammonia T6 (n-6 to n chamber)		*B. marginata* (n-3 to n chamber)		*C. laevigata* (n-2 to n chamber)	
	Sr/Ca	Mg/Ca	Sr/Ca	Mg/Ca	Sr/Ca	Mg/Ca
r	0.189	−0.136	0.026	−0.074	0.081	−0.119
p	0.0002	0.009	0.664	0.216	0.353	0.173

(cf. SEM images Supplementary material S5).

Amongst the total *Ammonia* T6 specimens cultured in our experiment, ~ 68% calcified between one and five chambers, and ~ 16% between six and eleven chambers (cf. details in Fig. 3a). For some specimens of *C. laevigata* and *B. marginata* that calcified only one chamber, the identification of the newly calcified chamber under epifluorescence microscope was problematic. This was because the fluorescence of the old calcein-labelled chambers (i.e., not formed during our experiment) reflected on the last one (i.e., formed during our experiment), which explains the presence of doubtful chambers (~ 2% on average for *B. marginata* and ~ 10% for *C. laevigata*; cf. "1?" in Figs. 3b; c). Amongst the total *B. marginata* specimens cultured in our experiment, ~ 18% on average calcified one to two chambers and ~ 2% three to five chambers. For *C. laevigata*, ~ 5% calcified one chamber and only ~ 1% calcified two chambers. There is no clear pattern in terms of the number of calcified chambers between the eight experimental conditions for each species (Fig. 3).

3.3. Link between foraminiferal Sr/Ca and C-system

To analyze the correlation between foraminiferal Sr/Ca for each species and the individual C-system parameters, linear regression analyses were first performed using data from both set-ups A and B. The results of the regression analyses (intercepts and slopes) and the statistical outputs (p, and R^2) are summarized in Table 3. For *Ammonia* T6 and *B. marginata*, all the regressions were strongly significant ($p < 0.05$), except for Sr/Ca$_{B. marginata}$ vs. pH and explained, depending on the C-system parameter, between 5% and 53% of the observed variability in

Sr/Ca. For *C. laevigata*, although the regressions were significant ($p < 0.05$) except for Sr/Ca$_{C. laevigata}$ vs. pCO$_2$ and pH, they only explained 6% of the observed variability in Sr/Ca.

To narrow down the main controlling parameters, Fig. 4 presents linear regression models for each set-up and the results of the regression analyses (intercepts and slopes) and the statistical outputs (p, and R^2) are summarized in Table 3. The results of *Ammonia* T6 and *B. marginata* showed significant correlations ($p < 0.05$) in set-up B between Sr/Ca and all the measured parameters. These correlations present a high R^2 (>0.60), except for pH. Significant correlations ($p < 0.05$) were also found in set-up A between Sr/Ca and all the measured parameters for *Ammonia* T6, although with lower R^2 (<0.24). For *B. marginata*, no significant correlations ($p < 0.05$) were found in set-up A with any of the C-system parameters except for the DIC but with a very weak R^2 ($= 0.04$). For TA, DIC and [HCO$_3^-$], all data points from set-up A fall on the regression lines of set-up B. For *C. laevigata*, no trends were recorded between Sr/Ca and individual parameters of the C-system.

The ANCOVA tests analyses showed no significant difference between intercepts of *Ammonia* T6 regression models (Sr/Ca vs [HCO$_3^-$] and DIC) in our study and that of Keul et al. (2017) ($F = 2.1$, $p = 0.15$), but shows a significant difference in the slopes ($F = 40.4$, $p = 3.8 \ 10^{-10}$) (Table 4). The ANCOVA tests analyses showed a significant difference between intercepts of *Ammonia* T6 and *B. marginata* (this study) regression models ($F = 200.7$, $p = 8.7 \ 10^{-40}$). There was a statistically significant, but weak, difference between the slopes of the two species ($F = 5.4$, $p = 0.02$) (Table 4).
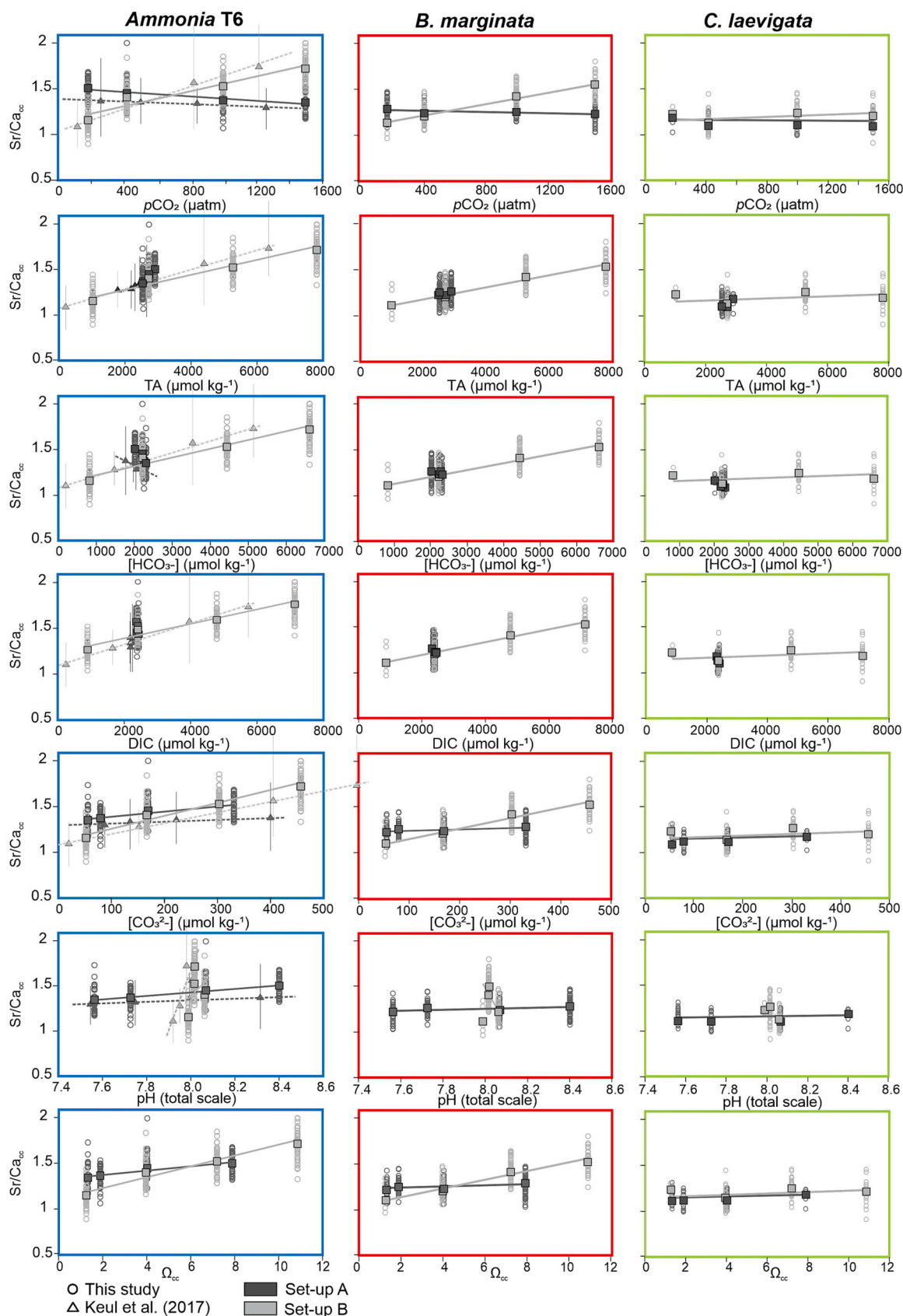
Fig. 4. Foraminiferal Sr/Ca (mmol mol^{-1}) versus individual C-system parameters for *Ammonia* T6, *B. marginata* and *C. laevigata*. Squares represent the mean values. Lines represent linear regressions. *Ammonia* T6 data from the study of Keul et al. (2017) are plotted with *Ammonia* T6 from this study. The error bars in the data of Keul et al. (2017) represent the maximum dispersion of points around the means (triangles). Dashed lines represent linear regressions.

3.4. Variability in Sr/Ca and Mg/Ca ratios between chamber stages and replicates

Here we evaluate the ontogenetic effect based on chamber stages since we did not obtain reproduction. For *Ammonia* T6, we estimated that adding on average five to six chambers increased the diameter from ~ 150 to 250 μm. For *B. marginata*, adding on average two to three chambers increased the maximum length from ~ 150 to 300 μm. For *C. laevigata*, adding on average one chamber increased the diameter from ~ 150 to 200 μm (cf. supplementary material S1).

To evaluate a potential ontogenetic effect (chamber stages) on Sr and Mg incorporation, we present in Fig. 5 the average of Sr/Ca and Mg/Ca ratios calculated for the different chambers of each species. In Supplementary material S6, we present the same results for Sr/Ca displayed for each condition. The Spearman's rank-order correlation coefficients calculated between these ratios and the position of the newly formed chambers, all treatments combined (Table 5), showed no significant correlations for *B. marginata* and *C. laevigata* (p > 0.05) and significant correlations for *Ammonia* T6 (p > 0.05) but with very low coefficients (r = 0.18 and − 0.13 for Sr/Ca and Mg/Ca respectively). This indicates the absence of ontogenetic trends in Sr/Ca and Mg/Ca ratios. Caution should be taken for *B. marginata* and *C. laevigata* that calcified fewer chambers compared to *Ammonia* T6.

In Fig. 6a and b, we plotted Sr/Ca ratios against Mg/Ca ratios by species and pseudo-replicate, using respectively all measurements, and average data from each experimental condition. The results demonstrated that *Ammonia* T6 had higher Sr/Ca ratios and lower Mg/Ca ratios than the two other species showing equivalent absolute El/Ca values. There was also no significant correlation between Sr/Ca and Mg/Ca ratios for each species. The variability of Sr/Ca in *Ammonia* T6, *B. marginata* and *C. laevigata* (relative standard errors of 1.4, 1.3 and 2% on average, respectively) was much smaller than the variability observed in Mg/Ca (relative standard errors of 19.1, 11.3 and 12.4% on average, respectively).

Figs. 6 (c-e) presents box plots of Sr/Ca and Mg/Ca ratios per species and pseudo-replicate, considering the eight experimental conditions together. In general, the results displayed similar values between replicates for each species. Statistical analyses showed however a significant difference (p = 0.01) between Sr/Ca values in R_{net} and R1 for *Ammonia* T6 but since there was no significant difference between R_{net} and R2, we cannot conclude on an effect of the covering net. For *C. laevigata*, Sr/Ca values in R_{net} were significantly different from R1 and R2 but with p values close to 0.05, meaning that the difference was very low. For Mg/Ca ratios in the same species, R2 was significantly different from R_{net} and R1.
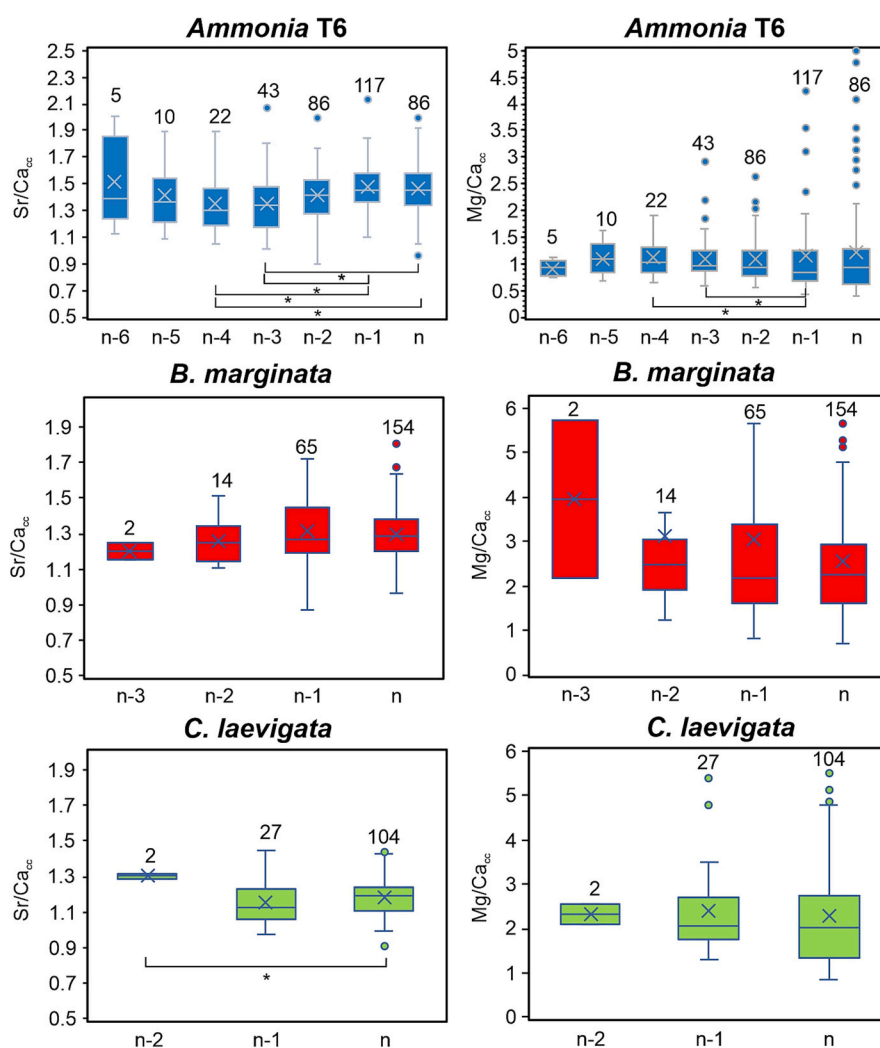

Fig. 5. Box plots showing Sr/Ca and Mg/Ca ratios (mmol mol^{-1}) measured in foraminiferal calcite as a function of the position of the newly formed chambers; "n-6" being the oldest and "n" the last chamber formed. The number of data points is indicated on top of the histograms. The pairwise significant differences (p < 0.05) are indicated with a bracket and an asterisk (Kruskal Wallis test).
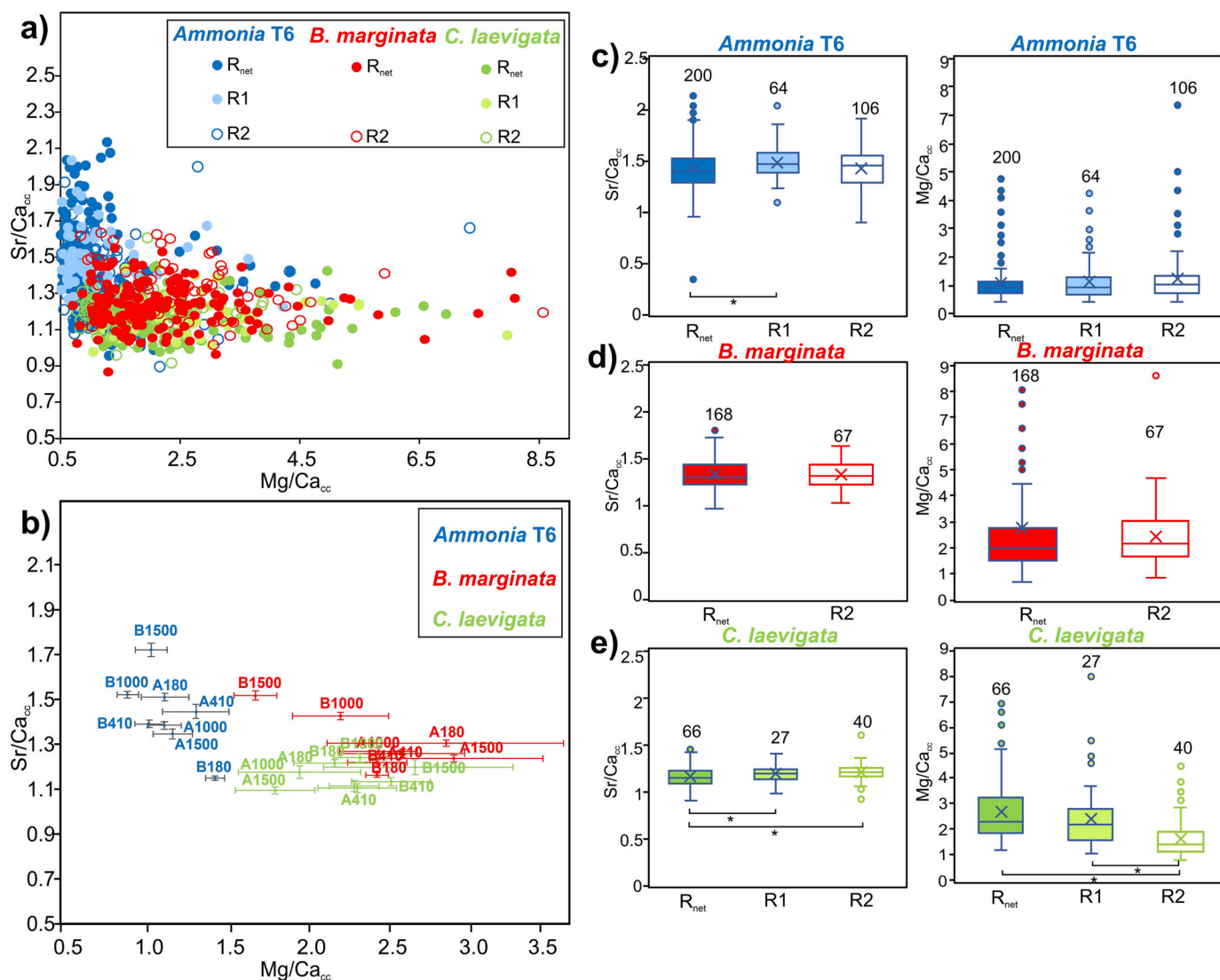
Fig. 6. Sr/Ca and Mg/Ca (mmol mol^{-1}) measured in the calcite formed in the experiment of the three cultured benthic species. a) all data points from the eight treatments and different pseudo-replicates are plotted together, b) average values per treatment. Error bars correspond to standard errors. (c-e) Sr/Ca and Mg/Ca plotted for each replicate and each cultured species. The number of data points is indicated on top of the box plots. The pairwise significant differences (p < 0.05) are indicated with a bracket and an asterisk (Kruskal Wallis test).

4. Discussion

4.1. Survival and growth of benthic foraminifera

Many specimens of the three cultured benthic species survived and calcified new chambers in the eight controlled conditions, with however higher survival and growth percentages for *Ammonia* T6 compared to the two other species studied (Fig. 2). It is well known that shallow-water foraminifera adapt more easily (growth and reproduction) to laboratory cultures (e.g., Raitzsch et al., 2010; Dueñas-Bohórquez et al., 2011b; van Dijk et al., 2019; Geerken et al., 2022) than most deep-sea species. This is likely because shallow-water taxa have a natural adaptability to stressful and variable conditions characterizing their natural environments (e.g., variable salinity and temperature) (e.g., Bradshaw, 1961; Murray, 1991; Pascal et al., 2008; Geslin et al., 2014) whereas deep-sea species live in more stable settings (e.g., high pressure, stable salinity, and temperature). Unlike many other deep-sea foraminiferal taxa, *B. marginata* usually shows a rather good adaptation to laboratory conditions (e.g., Barras et al., 2009, 2010, 2018; Filipsson et al., 2010; Wit, 2012; Geslin et al., 2014; Nardelli et al., 2014).

Cassidulina laevigata has only been used to a limited extent in culture studies and it has typically low tolerance to anoxic conditions (e.g., Nardelli et al., 2014).

Amongst the eight controlled conditions, we expected possible negative effects (i.e., decalcification, reduced growth) on the cultured species under low pH conditions A1000 (pH = 7.73) and A1500 (pH = 7.56). Instead, no difference (according to Dixon's test) was observed compared to most other conditions with "normal" or high pH values (Fig. 3). Responses of calcifying benthic foraminifera to pH changes are not consistent and laboratory studies show that calcification/dissolution rates under varying pH concentrations differ between and within species. Guamán-Guevara et al. (2019) report increased mortality of *Elphidium williamsoni* under low pH conditions (7.3 ≤ pH ≤ 7.7), and Charrieau et al. (2018) further document severe decalcification for *Ammonia* sp. and *Elphidium crispum* (7.25 ≤ pH ≤ 7.5). Several studies observe continuing growth under low pH conditions while reporting a reduction in shell weight, size or the number of newly added chambers in several species, including *Ammonia* group *tepida* (e.g., Dissard et al., 2010a; Knorr et al., 2015; Prazeres et al., 2015; Guamán-Guevara et al., 2019; Oron et al., 2020). On the contrary, other studies do not report any

low pH-related negative effects on several species of benthic forami-nifera, including *B. marginata* (e.g., McIntyre-Wressnig et al., 2013, 2014; Haynert et al., 2014; Wit et al., 2016; Weinmann et al., 2021). While enhanced dissolution due to acidification is mainly an inorganic process, Toyofuku et al. (2017) suggest that the calcification in some species might be largely unaffected by decreasing pH as they find, together with other studies (e.g., Glas et al., 2012), that *Ammonia* sp. reduces its surrounding pH during chamber formation until 6.9 and even 6.3. Our results are in line with these findings, suggesting that there is a strong organismal control over biomineralisation during foraminiferal calcification that possibly makes them more adaptive and robust in coping with acidification (e.g., Toyofuku et al., 2017; Kawahata et al., 2019). While this is certainly true for *Ammonia* T6 showing successful calcification in most conditions ($> 80\%$ of the cultured specimens calcified), caution should be taken for the two deep-sea species of which only $\sim 20\%$ of the specimens grew in culture. It is therefore possible that the minority that did calcify were also those able to withstand/resist the varying pH conditions. Still, the survival and growth percentages that we recorded for *B. marginata* for example are in line with other culture experiments (e.g., $\sim$ 30–40% and 15–30%, respectively; Geslin et al., 2014), meaning that this is a common feature in culture regardless of the controlled parameters. For a broader perspective, the fact that the studied species calcified well under low pH conditions might be coherent with geological records showing the resistance of some species to high pCO$_2$ time periods (e.g., Foster et al., 2013), although these occurred over evolutionary timescales, and were associated with a covariance in other factors.

In the low DIC condition B180 (DIC = 880 µmol kg^{-1}, TA = 1029 µmol kg^{-1}), characterized by a normal pH (7.99), *B. marginata* and *C. laevigata* calcified fewer chambers (Fig. 3b-c). *Ammonia* T6, however, did not show any significant difference compared to most other "normal" or high DIC conditions (Fig. 3a). These results seem to indicate a higher vulnerability of the two deep-sea species to low DIC concen-trations than the shallow water species *Ammonia* T6 (Fig. 3a). Yet, Keul et al. (2013) report the lowest growth rate and size-normalized weight of *Ammonia* T6 under low DIC conditions (246 µmol kg^{-1}), although lower than in our case study. This might indicate a DIC threshold value below which *Ammonia* struggles to calcify. Additionally, and only in the R$_{net}$ replicate of the B180 condition, the three species showed severe signs of dissolution (Supplementary material S5), especially for *B. marginata* and *C. laevigata* specimens that were very fragile and sometimes broke during manipulation. This indicates that the net aggravated the impact of low DIC seawater on benthic foraminifera, most likely by creating a more isolated micro-environment where the seawater DIC is depleted faster.

One could argue that we decreased/increased the seawater DIC in our experiment beyond typical modern values in the ocean ($\sim$ 1800–2300 µmol kg^{-1}; e.g., Wu et al., 2019). This is first justified by the fact that low/high DIC concentrations were probably encountered in the past in open marine waters during specific climatic periods (e.g., Vigier et al., 2015; Zeebe and Tyrrell, 2019), although the recent re-constructions of Zeebe and Tyrrell (2019) suggest that long-term DIC and TA were similar to modern values across the past 100 Myr regardless of the varying atmospheric pCO$_2$. Furthermore, in coastal waters, the carbonate chemistry is substantially more dynamic than the open ocean due, amongst others, to seasonal fluctuations and freshwater discharges (e.g., Borges and Gypens, 2010; Rheuban et al., 2019). The DIC and TA of near-river waters are largely governed by the type of bedrock of the catchment area, with high values ($>$3000 µmol kg^{-1}) associated with limestone or carbonate bedrock and low values ($<$1000 µmol kg^{-1}) linked to sandstones and volcanic rocks (e.g., McGrath et al., 2016). Additionally, there is a close connection to salinity, especially for waters with low DIC and TA concentrations that increase with increasing salinity in the outer estuary (e.g., McGrath et al., 2016). As such, and unlike deep-sea species, the low vulnerability of the intertidal *Ammonia* T6 to low DIC concentrations in our experiment might be due to

organismal adaptability in its natural environment with variable salin-ities and freshwater input.

4.2. Effect of the C-System on Sr incorporation

Our results showed that Sr/Ca in *Ammonia* T6 and *B. marginata* vary in a similar fashion (i.e., trends) with respect to the C-system parameters as the Sr/Ca in *Ammonia* T6 of Keul et al. (2017) grown in a comparable decoupled C-system experiment (Fig. 4). In the decoupled C-system study of van Dijk et al. (2017b), Sr/Ca values of *Ammonia* T6 did not show any correlation with the C-system. However, when considering the partition coefficient (D$_{Sr}$), van Dijk et al. (2017b) found similar trends (Supplementary material S7). Because Sr/Ca in foraminifera correlates with Sr/Ca$_{sw}$ (e.g., Langer et al., 2016), the discrepancy in the trends between Sr/Ca and D$_{Sr}$ in the study of van Dijk et al. (2017b) might be due to the unstable Sr/Ca$_{sw}$ values between the experimental conditions (4.4–6.4 mmol mol^{-1}) (cf. additional discussion in Supplementary ma-terial S8). The overall consistency between the results issued from comparable C-system experiments validates the positive correlation between foraminiferal Sr/Ca and the C-system, at least for *Ammonia* T6 and *B. marginata*. However, caution should be taken in paleo-applications with respect to spatio-temporal Sr/Ca$_{sw}$ variability (e.g., Lebrato et al., 2020), even on time-scales shorter than Sr residence time in seawater ($\sim$3 Myrs; Richter and Turekian, 1993).

Sr/Ca ratio in *C. laevigata* did not record any C-system dependency (Fig. 4), even though we had a conservative approach by discarding the Sr/Ca values of the doubtful chambers from the calculation of regression models. We can hypothesize that this species poorly tolerated our lab-oratory conditions (e.g., lack of sediment, high range of pH and DIC, etc.). This might have resulted in a physiological stress that impacted biomineralisation pathways and incorporation of Sr into the calcite. We can also assume a strong species-specific effect, affecting not only the nature of the correlation with the forcing parameter (e.g., slope, inter-cept, linear, exponential, etc.), such as in the case of Mg/Ca vs tem-perature (e.g., Toyofuku et al., 2000; Lowenstein and Hönisch, 2012), but also the existence/absence of such relationship (i.e., the mechanism that drives the Sr/Ca - C-System relationship in the other species is not present in *C. laevigata*). Such a drastic species-specific effect would be an issue for paleo-reconstructions based on foraminiferal Sr/Ca since typically culture calibrations are based on very few species and the re-sults are extrapolated to other species hypothesizing that, although the absolute values change, the relative response to the environmental parameter would be similar. Based on that, Mojtahid et al. (2017) hy-pothesized that the low Sr/Ca in *C. laevigata* recorded during the last Heinrich event ($\sim$ 16.5 cal ka BP) indicated a change in water mass carbonate chemistry in the northeast Atlantic. Based on our findings, this hypothesis might not be valid. Instead, the recorded anomaly in Sr/Ca in *C. laevigata* might indicate a small-scale change of Sr/Ca$_{sw}$, devi-ating from seawater Sr conservative behavior (e.g., Lebrato et al., 2020). More experimental and core top studies involving *C. laevigata* should help elucidating the observed deviation and confirm whether it is a common pattern for *C. laevigata* once put in laboratory conditions, or whether this was specific to our experimental conditions.

4.3. DIC and/or [HCO$_3^-$] as the main controlling factors for Sr/Ca ratio

We can assume that if a certain C-system parameter is controlling incorporation of Sr into foraminiferal calcite, the correlation between Sr/Ca and this parameter should be similar in both set-ups A and B. As such, for *Ammonia* T6 and *B. marginata*, we can exclude pCO$_2$, [CO$_3^{2-}$] and Ω$_{cc}$ (Fig. 4). pH can also be excluded because, although a trend can be observed in treatment A, the R^2 value is very small (Fig. 7a; Table 3) indicating that there is no predictive power of pH on foraminiferal Sr/Ca. This leaves us with [HCO$_3^-$], TA and DIC as potential controlling factors. In set-up A (i.e., stable DIC), all [HCO$_3^-$] and TA values fall within a narrow range, which is not surprising since HCO$_3^-$ is the major
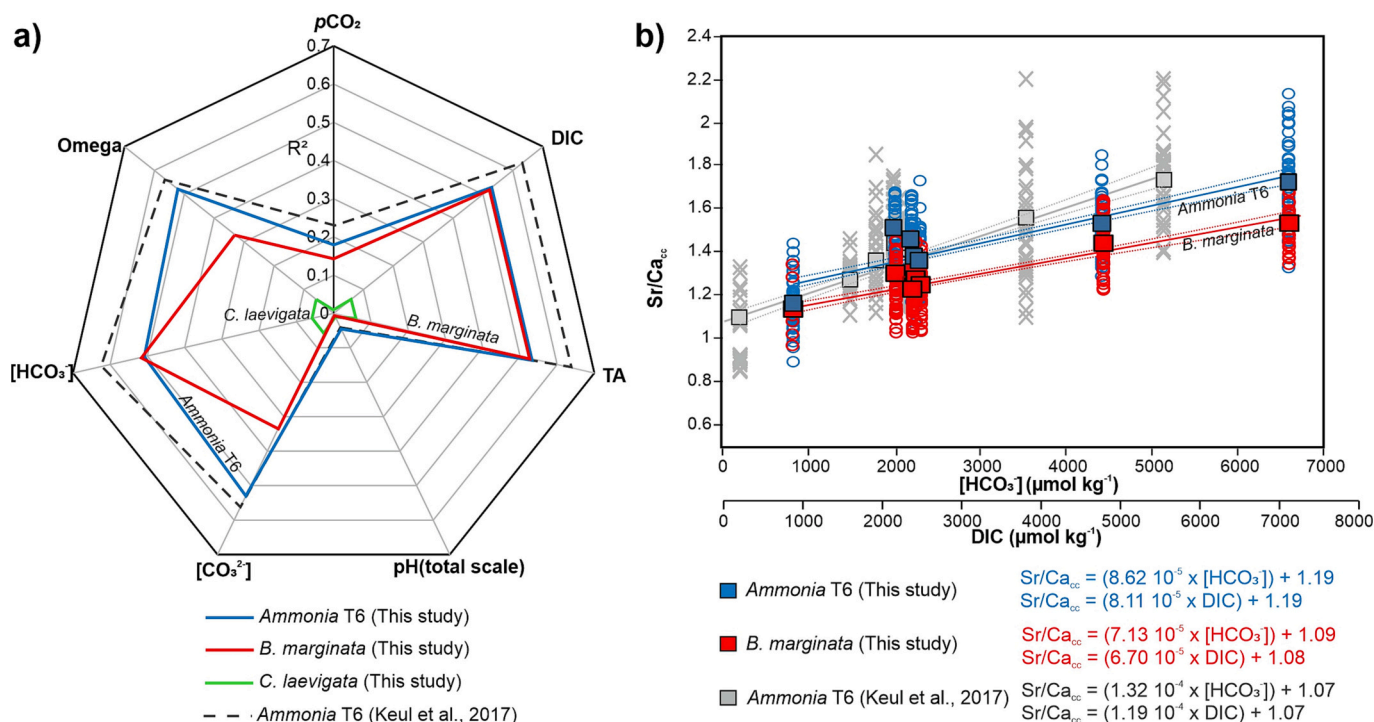
Fig. 7. Linear regression analyses. a) radar chart representing the R^2 values of the regression analyses between foraminiferal Sr/Ca and respective C-system parameters. The R^2 values reported by Keul et al. (2017) are also plotted, b) Calibration equations of foraminiferal Sr/Ca vs [HCO$_3^-$] and DIC for our study and the study of Keul et al. (2017). Linear regression parameters of the calibration equations from the study of Keul et al. (2017) were recomputed from raw data because of an error in the publication. The dotted lines represent 95% confidence level.

constituent of both TA and DIC. Despite the narrow range of values, we can observe a decreasing trend of Sr/Ca with the slight increase in [HCO$_3^-$] in set-up A for *Ammonia* T6, oppositely to set-up B (Fig. 4). However, because the R^2 value is very small, and because this trend is not existent for *B. marginata* (Table 3), we cannot exclude [HCO$_3^-$]. Furthermore, since all [HCO$_3^-$] and TA values from set-up A fall overall on the regression line of set-up B (Fig. 4), this means that [HCO$_3^-$], TA and/or DIC might control Sr/Ca incorporation (high R^2 values; Fig. 7a). The data presented here cannot empirically disentangle the effects of these parameters. However, because TA has no "physical reality" which could be used by an organism, we can narrow it down to DIC and/or [HCO$_3^-$] as the main driving forces behind the Sr incorporation in the calcite of *Ammonia* T6 and *B. marginata*. This is in line with the conclusions of Keul et al. (2017) for *Ammonia* T6.

When plotting Sr/Ca values against DIC and [HCO$_3^-$] for *Ammonia* T6 and *B. marginata*, the regression models were overall similar and consistent with that published by Keul et al. (2017) for *Ammonia* T6 (Fig. 7b). Furthermore, there was no significant difference between the intercepts of *Ammonia* T6 regression models from both studies (Table 4). Though, a significant difference in the slopes was found and might be explained either by i) slight instabilities in the chemical system of Keul et al. (2017) (e.g., differences between nominal and measured pCO$_2$ and between set-ups A and B) that we were able to improve thanks to the Ecolab system, or ii) by the fact that the DIC ranges were slightly different, with Keul et al. (2017) reaching lower DIC values than in our experiment. The regression models of *Ammonia* T6 and *B. marginata* (this study) showed overall parallel trends but a significant offset between the main values of Sr/Ca (Fig. 7b). This is a common feature in most elemental incorporation in foraminiferal test during calcification, due to biological processes that are often species dependent (e.g., Toyofuku et al., 2011; van Dijk et al., 2017a; Barras et al., 2018). This means that there is a species-specific effect that will affect absolute values estimations (i.e., different intercept) in paleo-reconstructions but not the relative DIC and/or [HCO$_3^-$] variations (i.e., similar slope). That said,

and although the trends observed here are robust, the sensitivity of the Sr/Ca to DIC and/or [HCO$_3^-$] seems to be low (~ 0.04 mmol mol^{-1}/500 µmol kg^{-1} DIC), and as such, it does not form a strong paleo-proxy, especially for small shifts in these parameters. This low sensitivity, however, can be partly counterbalanced by the fact that Sr is analytically robust (e.g., Dueñas-Bohórquez et al., 2011a; de Nooijer et al., 2014), and with very little inter- and intra-individual variability as discussed in section 4.4.

Keul et al. (2017) explored the transmembrane transport model to explain the impact of DIC and/or [HCO$_3^-$] on Sr/Ca in *Ammonia* T6. According to these authors, pCO$_2$ and HCO$_3^-$ enter the biomineralisation space (i.e. site of calcification), created by the pseudopodial network (i. e., protective envelop), where they are converted to CO$_3^{2-}$. Keul et al. (2017) further hypothesized that in order to keep Ω constant, foraminifera have to decrease Ca causing increasing Sr/Ca in the calcite (Keul et al., 2017). Alternatively, Toyofuku et al. (2017) emphasized that HCO$_3^-$ is externally transformed into CO$_2$ due to active proton pumping, meaning that biomineralisation does not rely on the availability of CO$_3^{2-}$. Once inside the biomineralisation space, calcification is driven by rapid transformation of CO$_2$ into CO$_3^{2-}$ due to the high pH sustaining CaCO$_3$ precipitation by reacting with Ca^{2+} (Toyofuku et al., 2017). Therefore, we can suppose that the more DIC and/or HCO$_3^-$ is available, the more CO$_2$ diffuses inside the biomineralisation space, which will increase precipitation rate of calcite. This has been shown for inorganic precipitation of calcite, where the rate increases with increasing DIC and with it Sr incorporation into calcite (e.g., Lorens, 1981; AlKhatib and Eisenhauer, 2017). We can suppose that this mechanism might be responsible for higher Sr/Ca ratios in foraminiferal calcite at higher DIC and/or HCO$_3^-$ concentrations. Alternatively, if we consider the seawater vacuolization model (i.e., closed pool of seawater) (e.g., Erez, 2003; Evans et al., 2018), when there is more DIC, potentially more calcite can be formed necessitating utilizing more of the Ca pool, resulting in higher Sr/Ca ratio in foraminiferal shells. Mean D$_{Sr}$ values in the present study for the three species (~ 0.13–0.21 mmol mol^{-1}) plot near the highest D$_{Sr}$

values measured for inorganic precipitation calcite (e.g., 0.02–0.14; Lorens, 1981; Tesoriero and Pankow, 1996; Nehrke et al., 2007), meaning probably a non-negligible role of inorganic processes (i.e., a relatively weak biological control) as hypothesized by Evans et al. (2018).

To test whether other divalent cations display the same relationship to DIC and/or [HCO_3^-], we measured alongside with Sr/Ca in *Ammonia* T6, Ba/Ca, Zn/Ca and Mg/Ca and in *B. marginata*, Mg/Ca. None of these ratios showed a relationship with any of the C-system parameters (Supplementary material S9). This may imply other biomineralisation pathways for these specific elements. Although it was only possible to measure Mg/Ca$_{sw}$ ($\sim$ 5260 mmol mol^{-1}) in our culture study, it is well known that, in contrast to D$_{Sr}$, perforate foraminifera D$_{Zn}$ and D$_{Mg}$ are below inorganic calcite values (e.g., Rosenthal et al., 1997; van Dijk et al., 2017b), meaning a high discrimination against Zn and Mg by exerting perhaps a strong biological control. Moreover, van Dijk et al. (2017b) showed that Zn/Ca in *Ammonia* T6 decreased with increasing [CO_3^{2-}]. Because we used a similar decoupled experiment as van Dijk et al. (2017b), this discrepancy can partly be explained by the fact that Zn concentration of the culture media in the study of van Dijk et al. (2017b) was increased by $\sim$15 times compared to open ocean seawater [Zn]. Some studies reported a certain link between Mg/Ca and the C-system, but this link is not systematic, especially for the *Ammonia* group *tepida*, where several culture studies show no effect of the carbonate chemistry on Mg/Ca (e.g., Dissard et al., 2010a, 2010b; Dueñas-Bohórquez et al., 2011b; Allison et al., 2011; van Dijk et al., 2017b). It appears therefore that the mechanisms responsible for the partitioning against Mg and Zn have very different sensitivities to certain key parameters than the mechanisms responsible for Sr incorporation. Foraminiferal D$_{Ba}$, on the other hand, lies on the high side of the range of inorganic precipitation (Lea and Spero, 1994), similarly to Sr and in consistency with inorganic calcite precipitation according to Evans et al. (2018). Following the same logic, Sr and Ba should display similar relationships to the C-system. Yet, in symbiont-bearing high Mg content hyaline tropical foraminifera, van Dijk et al. (2017a) reported the same behavior of Zn and Ba with increasing *p*CO$_2$, and concluded that their incorporation in foraminiferal calcite might be depending on the availability of free ions and the formation of carbonate complexes, unlike the unaffected Sr/Ca since the availability of Sr^{2+} does not change with *p*CO$_2$. This shows the high complexity and variety of possible biomineralisation pathways that seem to differ between species, and for each element. More decoupled C-system experimental studies with benthic foraminifera are necessary to test and refine the proposed biomineralisation models.

4.4. Sr/Ca and Mg/Ca ratios between and within specimens and species

Despite stable culturing conditions, the variability observed in Sr/Ca ratios between and within specimens (relative standard errors of 1.4, 1.3 and 2% on average) was much smaller than the variability observed in Mg/Ca ratios (relative standard errors of 19.1, 11.3 and 12.4% on average) for *Ammonia* T6, *B. marginata* and *C. laevigata* respectively (Fig. 6). This is in line with previous findings showing generally uniform Sr/Ca ratios within the carbonate tests of foraminifera compared to Mg/Ca and seems to be inherent to the process of bio-calcification itself in the incorporation of these two elements (e.g., Eggins et al., 2003; Dueñas-Bohórquez et al., 2011a; de Nooijer et al., 2014) and the potential Mg-related diagenetic contamination even in the inner layers of the calcite for fossil specimens (e.g., Sexton et al., 2006; Schneider et al., 2017). This implies that Sr is analytically very robust, with high accuracy and precision (i.e., only few ablation spots are sufficient to estimate the average with low uncertainty), not easily contaminated, and more importantly with little variability in the shells.

To test for a potential ontogenetic effect on Sr and Mg incorporation into foraminiferal tests, and since we did not obtain reproduction allowing to investigate different size fractions, we analyzed the ratios in the successive chambers in single specimens. No detectable ontogenetic effect was observed in Sr/Ca and Mg/Ca ratios for the last chamber stages of the three studied species (Fig. 5; Table 4), suggesting that i) there was no significant chamber stage-related impact on Sr/Ca and Mg/Ca within the growth range obtained ($\sim$ 150–300 μm) and ii) precipitation rates were probably similar during production of the last chambers. This in line with Geerken et al. (2022) who showed, using Sr-labeling, that precipitation rate is uniform amongst specimens and within chamber walls *of Ammonia beccarii*. Our results strongly suggest that we can exclude possible effects of ontogeny, at least between different chamber stages, to explain the differential incorporation of Sr/Ca in our experimentation, which is crucial for paleo-reconstructions of the C-system. For *Ammonia* spp. and *Bulimina* spp., the lack of ontogenetic trends in foraminiferal Sr/Ca and Mg/Ca has been reported in several studies investigating this effect in successive chambers in single specimens (e.g., Wit et al., 2012; de Nooijer et al., 2014). Some studies also report a lack of ontogenetic trend in Sr/Ca and Mg/Ca of *Bulimina* spp. between individual specimens from different size fractions (e.g., $\sim$ 100–500 μm, 300–600 μm; Hintz et al., 2006; Wit et al., 2012, respectively), whereas Diz et al. (2012) report a size-related trend Sr/Ca for *Ammonia* sp. between 150 and 600 μm in size. However, when considering only sizes between 150 and 250 μm in the study of Diz et al. (2012), equivalent to the approximate range of growth of *Ammonia* T6 in our study (adding on average 5 to 6 chambers), the trend is no longer clear. For application of Sr/Ca ratios in paleostudies, this may imply that measurements can be performed regardless of the chamber stage in single specimens, using laser ablation or even bulk analyses, provided the use of a restricted size fraction.

Amongst the three species, *Ammonia* T6 recorded the highest Sr/Ca ratios on average and the lowest Mg/Ca ratios (Fig. 6a; b). Lower incorporation of Mg by *Ammonia* spp. than *Bulimina* spp. is a common feature reported in several studies (e.g., Dissard et al., 2010b; Filipsson et al., 2010; Toyofuku et al., 2011; Wit et al., 2012; Groeneveld et al., 2018). This seems also to be the case for other elements such as Mn (Barras et al., 2018). In our case study, this feature seems to be inversed for Sr between *Ammonia* T6 and *B. marginata*. Several studies argue that Sr/Ca of foraminiferal calcite is associated with increased shell Mg content, distorting the calcite lattice and weakening the discrimination against Sr (e.g., Mewes et al., 2015; Langer et al., 2016; Yu et al., 2019). Yet, our results showed no significant correlation between Mg/Ca$_{cc}$ and Sr/Ca$_{cc}$ ratios for the three cultured species (Fig. 6a; b). It is possible that the close relationship between Sr incorporation and Mg content is only robust for high Mg content species (e.g., large tropical hyaline foraminifera) vs low Mg species (e.g., temperate small benthic foraminifera) (van Dijk et al., 2017a), and not systematic within the low Mg group. The absence of correlation between Sr/Ca and Mg/Ca values for our low Mg species seems to confirm that the mechanism responsible for the partitioning against Mg is sensitive to other factors than that for Sr incorporation. This has been also hypothesized for the planktonic foraminifer *G. sacculifer* (e.g., Dueñas-Bohórquez et al., 2011a).

5. Conclusions

- Growth and survival of *Ammonia* T6, *B. marginata* and *C. laevigata* were unaffected by a pH as low as 7.5 under open marine-like DIC and TA conditions. However, at a normal pH ($\sim$ 8.0), growth of *B. marginata* and *C. laevigata* was negatively impacted by low DIC conditions (879 μmol kg^{-1}). The absence of such an impact on *Ammonia* T6 growth demonstrates the high tolerance of this shallow water species to extreme DIC conditions, probably as a result of its variable natural environment. The decoupling of DIC and pH impacts are in line with the transport of CO$_2$ to the site of calcification as proposed in Toyofuku et al. (2017).

- There was a clear positive correlation between foraminiferal Sr/Ca and the C-system for *Ammonia* T6 and *B. marginata*. Sr/Ca ratio in *C. laevigata* however did not record any C-system dependency. We hypothesized either i) a strong species-specific effect that should be

considered in paleo-studies or ii) a poor tolerance to laboratory conditions which resulted in a physiological stress that impacted Sr incorporation.

- Our results confirmed that DIC and/or [HCO_3^-] are the driving forces behind Sr incorporation in the calcite of *Ammonia* T6 and *B. marginata*. The regression models showed similar slopes, confirming the reproducibility of such complicated experimentations, but different intercepts, suggesting that there is a species-specific effect between these two species that needs to be considered in paleo-applications. These paleo-applications would be limited by the low sensitivity of the Sr/Ca ratio to DIC and/or [HCO_3^-].

- The inter-chamber and inter-individual variability of Mg/Ca was larger than that of Sr/Ca for the three cultured species, which is in line with previous studies. No detectable ontogenetic effect was observed in Sr/Ca and Mg/Ca ratios for the last chamber stages of the three studied species. Hence, Sr/Ca is analytically robust, not easily contaminated, and measurements can be made regardless of the chamber stage (within a narrow size range), which can be advantageous for paleo-applications.

Supplementary data to this article can be found online at https://doi.org/10.1016/j.chemgeo.2023.121396.

Declaration of Competing Interest

None.

Data availability

Raw data is available on SEANOE data repository (https://doi.org/10.17882/89623).

Acknowledgments

References

AlKhatib, M., Eisenhauer, A., 2017. Calcium and strontium isotope fractionation in aqueous solutions as a function of temperature and reaction rate; I, Calcite. Geochim. Cosmochim. Acta 209, 296–319. https://doi.org/10.1016/j.gca.2016.09.035.

Allen, K.A., Hönisch, B., Eggins, S.M., Haynes, L.L., Rosenthal, Y., Yu, J., 2016. Trace element proxies for surface ocean conditions: a synthesis of culture calibrations with planktic foraminifera. Geochim. Cosmochim. Acta 193, 197–221. https://doi.org/10.1016/j.gca.2016.08.015.

Allison, N., Austin, H., Austin, W., Paterson, D.M., 2011. Effects of seawater pH and calcification rate on test Mg/Ca and Sr/Ca in cultured individuals of the benthic, calcitic foraminifera *Elphidium williamsoni*. Chem. Geol. 289, 171–178. https://doi.org/10.1016/j.chemgeo.2011.08.001.

Barras, C., Geslin, E., Duplessy, J.-C., Jorissen, F.J., 2009. Reproduction and growth of the deep-sea benthic foraminifer *Bulimina marginata* under different laboratory conditions. J. Foraminifer. Res. 39, 155–165. https://doi.org/10.2113/gsjfr.39.3.155.

Barras, C., Duplessy, J.C., Geslin, E., Michel, E., Jorissen, F.J., 2010. Calibration of δ18O of laboratory-cultured deep-sea benthic foraminiferal shells in function of temperature. Biogeosci. Discuss. 7, 335–350.

Barras, C., Mouret, A., Nardelli, M.P., Metzger, E., Petersen, J., La, C., Filipsson, H.L., Jorissen, F., 2018. Experimental calibration of manganese incorporation in foraminiferal calcite. Geochim. Cosmochim. Acta 237, 49–64. https://doi.org/10.1016/j.gca.2018.06.009.

Bijma, J., Pörtner, H.-O., Yesson, C., Rogers, A.D., 2013. Climate change and the oceans – what does the future hold?. In: Mar. Pollut. Bull., The Global State of the Ocean; Interactions Between Stresses, Impacts and Some Potential Solutions. Synthesis papers from the International Programme on the State of the Ocean 2011 and 2012 Workshops, 74, pp. 495–505. https://doi.org/10.1016/j.marpolbul.2013.07.022.

Boer, W., Nordstad, S., Weber, M., Mertz-Kraus, R., Hönisch, B., Bijma, J., Raitzsch, M., Wilhelms-Dick, D., Foster, G.L., Goring-Harford, H., Nürnberg, D., Hauff, F., Kuhnert, H., Lugli, F., Spero, H., Rosner, M., van Gaever, P., de Nooijer, L.J., Reichart, G.-J., 2022. A New Calcium Carbonate Nano-Particulate Pressed Powder Pellet (NFHS-2-NP) for LA-ICP-OES. Geostand. Geoanalytical Res, LA-(MC)-ICP-MS and μXRF. https://doi.org/10.1111/ggr.12425.

Borges, A.V., Gypens, N., 2010. Carbonate chemistry in the coastal zone responds more strongly to eutrophication than ocean acidification. Limnol. Oceanogr. 55, 346–353. https://doi.org/10.4319/lo.2010.55.1.0346.

Bradshaw, J.S., 1961. Laboratory experiments on the ecology of foraminifera. Cushman Found Foram Res Contr 12, 87–106.

Charrieau, L.M., Filipsson, H.L., Nagai, Y., Kawada, S., Ljung, K., Kritzberg, E., Toyofuku, T., 2018. Decalcification and survival of benthic foraminifera under the combined impacts of varying pH and salinity. Mar. Environ. Res. 138, 36–45. https://doi.org/10.1016/j.marenvres.2018.03.015.

de Nooijer, L.J., Hathorne, E.C., Reichart, G.J., Langer, G., Bijma, J., 2014. Variability in calcitic Mg/Ca and Sr/Ca ratios in clones of the benthic foraminifer *Ammonia tepida*. Mar. Micropaleontol. 107, 32–43. https://doi.org/10.1016/j.marmicro.2014.02.002.

Dickson, A.G., Sabine, C.L., Christian, J.R., 2007. Guide to Best Practices for Ocean CO2 Measurements (No. PICES Special Publication 3).

Dissard, D., Nehrke, G., Reichart, G.J., Bijma, J., 2010a. Impact of seawater pCO2 on calcification and Mg/Ca and Sr/Ca ratios in benthic foraminifera calcite: results from culturing experiments with *Ammonia tepida*. Biogeosciences 7, 81–93. https://doi.org/10.5194/bg-7-81-2010.

Dissard, D., Nehrke, G., Reichart, G.-J., Bijma, J., 2010b. The impact of salinity on the Mg/Ca and Sr/Ca ratio in the benthic foraminifera *Ammonia tepida*: results from culture experiments. Geochim. Cosmochim. Acta 74, 928–940. https://doi.org/10.1016/j.gca.2009.10.040.

Dixon, W.J., 1950. Analysis of Extreme Values. Ann. Math. Stat. 21, 488–506.

Dixon, W.J., 1951. Ratios Involving Extreme Values. Ann. Math. Stat. 22, 68–78. https://doi.org/10.1214/aoms/1177729693.

Diz, P., Barras, C., Geslin, E., Reichart, G.-J., Metzger, E., Jorissen, F., Bijma, J., 2012. Incorporation of Mg and Sr and oxygen and carbon stable isotope fractionation in cultured *Ammonia tepida*. Mar. Micropaleontol. 92–93, 16–28. https://doi.org/10.1016/j.marmicro.2012.04.006.

Dueñas-Bohórquez, A., da Rocha, R.E., Kuroyanagi, A., de Nooijer, L.J., Bijma, J., Reichart, G.-J., 2011a. Interindividual variability and ontogenetic effects on Mg and Sr incorporation in the planktonic foraminifer *Globigerinoides sacculifer*. Geochim. Cosmochim. Acta 75, 520–532. https://doi.org/10.1016/j.gca.2010.10.006.

Dueñas-Bohórquez, A., Raitzsch, M., de Nooijer, L.J., Reichart, G.-J., 2011b. Independent impacts of calcium and carbonate ion concentration on Mg and Sr incorporation in cultured benthic foraminifera. Mar. Micropaleontol. 81, 122–130. https://doi.org/10.1016/j.marmicro.2011.08.002.

Eggins, S., De Deckker, P., Marshall, J., 2003. Mg/Ca variation in planktonic foraminifera tests: implications for reconstructing palaeo-seawater temperature and habitat migration. Earth Planet. Sci. Lett. 212, 291–306. https://doi.org/10.1016/S0012-821X(03)00283-8.

Erez, J., 2003. The source of Ions for Biomineralization in Foraminifera and their Implications for Paleoceanographic Proxies. Rev. Mineral. Geochem. 54, 115–149. https://doi.org/10.2113/0540115.

Evans, D., Müller, W., Erez, J., 2018. Assessing foraminifera biomineralisation models through trace element data of cultures under variable seawater chemistry. Geochim. Cosmochim Acta 236, 198–217. https://doi.org/10.1016/j.gca.2018.02.048. Chemistry of oceans past and present: A Special Issue in tribute to Harry Elderfield.

Filipsson, H.L., Bernhard, J.M., Lincoln, S.A., McCorkle, D.C., 2010. A culture-based calibration of benthic foraminiferal paleotemperature proxies: δ18O and Mg/Ca results. Biogeosciences 7, 1335–1347. https://doi.org/10.5194/bg-7-1335-2010.

Fontanier, C., Jorissen, F.J., Chaillou, G., David, C., Anschutz, P., Lafon, V., 2003. Seasonal and interannual variability of benthic foraminiferal faunas at 550 m depth in the Bay of Biscay. Deep Sea Res. Part Oceanogr. Res. Pap. 50, 457–494. https://doi.org/10.1016/S0967-0637(02)00167-X.

Foster, L.C., Schmidt, D.N., Thomas, E., Arndt, S., Ridgwell, A., 2013. Surviving rapid climate change in the deep sea during the Paleogene hyperthermals. Proc. Natl. Acad. Sci. 110, 9273–9276. https://doi.org/10.1073/pnas.1300579110.

Ganopolski, A., Rahmstorf, S., 2001. Rapid changes of glacial climate simulated in a coupled climate model. Nature 409, 153–158. https://doi.org/10.1038/35051500.

Gattuso, J.-P., Epitalon, J.-M., Lavigne, H., Orr, J., 2019. Seacarb: seawater carbonate chemistry. In: R Package Version 3.2.12.

Geerken, E., de Nooijer, L., Toyofuku, T., Roepert, A., Middelburg, J.J., Kienhuis, M.V. M., Nagai, Y., Polerecky, L., Reichart, G.-J., 2022. High precipitation rates characterize biomineralization in the benthic foraminifer *Ammonia beccarii*. Geochim. Cosmochim. Acta 318, 70–82. https://doi.org/10.1016/j.gca.2021.11.026.

Geslin, E., Barras, C., Langlet, D., Nardelli, M.P., Kim, J.-H., Bonnin, J., Metzger, E., Jorissen, F.J., 2014. Survival, reproduction and calcification of three benthic foraminiferal species in response to experimentally induced hypoxia. In: Kitazato, H., Bernhard, J.M. (Eds.), Approaches to Study Living Foraminifera. Environmental Science and Engineering, Springer Japan, pp. 163–193.

Glas, M.S., Langer, G., Keul, N., 2012. Calcification acidifies the microenvironment of a benthic foraminifer (Ammonia sp.). J. Exp. Mar. Biol. Ecol. 424–425, 53–58. https://doi.org/10.1016/j.jembe.2012.05.006.

Groeneveld, J., Filipsson, H.L., Austin, W.E.N., Darling, K., McCarthy, D., Quintana Krupinski, N.B., Bird, C., Schweizer, M., 2018. Assessing proxy signatures of temperature, salinity, and hypoxia in the Baltic Sea through foraminifera-based geochemistry and faunal assemblages. J. Micropalaeontol. 37, 403–429. https://doi.org/10.5194/jm-37-403-2018.

Guamán-Guevara, F., Austin, H., Hicks, N., Streeter, R., Austin, W.E.N., 2019. Impacts of ocean acidification on intertidal benthic foraminiferal growth and calcification. PLoS One 14, e0220046. https://doi.org/10.1371/journal.pone.0220046.

Guillong, M., Meier, D.L., Allan, M.M., Heinrich, C.A., Yardley, B.W., 2008. SILLS: a MATLAB-based program for the reduction of laser ablation ICP-MS data of homogeneous materials and inclusions. Min. Assoc Can. Short Course Ser 40, 328–333.

Hammer, O., Harper, D.A.T., Ryan, P.D., 2001. PAST: Paleontological statistics software package for education and data analysis. Paleontol. Electron. 4 (1), 1–9.

Haynert, K., Schönfeld, J., Schiebel, R., Wilson, B., Thomsen, J., 2014. Response of benthic foraminifera to ocean acidification in their natural sediment environment: a long-term culturing experiment. Biogeosciences 11, 1581–1597. https://doi.org/10.5194/bg-11-1581-2014.

Hayward, B.W., Holzmann, M., Pawlowski, J., Parker, J.H., Kaushik, T., Toyofuku, M.S., Tsuchiya, M., 2021. Molecular and morphological taxonomy of living Ammonia and related taxa (Foraminifera) and their biogeography. Micropaleontology 67, 109–313. https://doi.org/10.47894/mpal.67.2-3.01.

Hintz, C.J., Shaw, T.J., Bernhard, J.M., Chandler, G.T., McCorkle, D.C., Blanks, J.K., 2006. Trace/minor element:calcium ratios in cultured benthic foraminifera. Part II: Ontogenetic variation. Geochim. Cosmochim. Acta 70, 1964–1976. https://doi.org/10.1016/j.gca.2005.12.019.

Hönisch, B., Hemming, N.G., Archer, D., Siddall, M., McManus, J.F., 2009. Atmospheric Carbon Dioxide Concentration across the Mid-Pleistocene transition. Science 324, 1551–1554. https://doi.org/10.1126/science.1171477.

Hönisch, B., Ridgwell, A., Schmidt, D.N., Thomas, E., Gibbs, S.J., Sluijs, A., Zeebe, R., Kump, L., Martindale, R.C., Greene, S.E., Kiessling, W., Ries, J., Zachos, J.C., Royer, D.L., Barker, S., Marchitto, T.M., Moyer, R., Pelejero, C., Ziveri, P., Foster, G. L., Williams, B., 2012. The Geological Record of Ocean Acidification. Science 335, 1058–1063. https://doi.org/10.1126/science.1208277.

Howes, E.L., Kaczmarek, K., Raitzsch, M., Mewes, A., Bijma, N., Horn, I., Misra, S., Gattuso, J.-P., Bijma, J., 2017. Decoupled carbonate chemistry controls on the incorporation of boron into Orbulina universa. Biogeosciences 14, 415–430. https://doi.org/10.5194/bg-14-415-2017.

Jochum, K.P., Weis, U., Stoll, B., Kuzmin, D., Yang, Q., Raczek, I., Jacob, D.E., Stracke, A., Birbaum, K., Frick, D.A., Günther, D., Enzweiler, J., 2011. Determination of Reference Values for NIST SRM 610–617 Glasses following ISO guidelines. Geostand. Geoanal. Res. 35, 397–429. https://doi.org/10.1111/j.1751-908X.2011.00120.x.

Kaczmarek, K., Langer, G., Nehrke, G., Horn, I., Misra, S., Janse, M., Bijma, J., 2015. Boron incorporation in the foraminifer Amphistegina lessonii under a decoupled carbonate chemistry. Biogeosciences 12, 1753–1763. https://doi.org/10.5194/bg-12-1753-2015.

Kawahata, H., Fujita, K., Iguchi, A., Inoue, M., Iwasaki, S., Kuroyanagi, A., Maeda, A., Manaka, T., Moriya, K., Takagi, H., Toyofuku, T., Yoshimura, T., Suzuki, A., 2019. Perspective on the response of marine calcifiers to global warming and ocean acidification—Behavior of corals and foraminifera in a high CO2 world "hot house.". Prog. Earth Planet. Sci. 6, 5. https://doi.org/10.1186/s40645-018-0239-9.

Keul, N., Langer, G., de Nooijer, L.J., Bijma, J., 2013. Effect of ocean acidification on the benthic foraminifera Ammonia sp. is caused by a decrease in carbonate ion concentration. Biogeosciences 10, 6185–6198. https://doi.org/10.5194/bg-10-6185-2013.

Keul, N., Langer, G., Thoms, S., de Nooijer, L.J., Reichart, G.-J., Bijma, J., 2017. Exploring foraminiferal Sr/Ca as a new carbonate system proxy. Geochim. Cosmochim. Acta 202, 374–386. https://doi.org/10.1016/j.gca.2016.11.022.

Knorr, P.O., Robbins, L.L., Harries, P.J., Hallock, P., Wynn, J., 2015. Response of the miliolid Archaias angulatus to simulated ocean acidification. J. Foraminifer. Res. 45, 109–127. https://doi.org/10.2113/gsjfr.45.2.109.

Langer, G., Sadekov, A., Thoms, S., Keul, N., Nehrke, G., Mewes, A., Greaves, M., Misra, S., Reichart, G.-J., de Nooijer, L.J., Bijma, J., Elderfield, H., 2016. Sr partitioning in the benthic foraminifera Ammonia aomoriensis and Amphistegina lessonii. Chem. Geol. 440, 306–312. https://doi.org/10.1016/j.chemgeo.2016.07.018.

Lea, D.W., Spero, H.J., 1994. Assessing the reliability of paleochemical tracers: Barium uptake in the shells of planktonic foraminifera. Paleoceanography 9, 445–452. https://doi.org/10.1029/94PA00151.

Lebrato, M., Garbe-Schönberg, D., Müller, M.N., Blanco-Ameijeiras, S., Feely, R.A., Lorenzoni, L., Molinero, J.-C., Bremer, K., Jones, D.O.B., Iglesias-Rodriguez, D., Greeley, D., Lamare, M., Paulmier, A., Graco, M., Cartes, J., Barcelos Ramos, J., de Lara, A., Sanchez-Leal, R., Jimenez, P., Paparazzo, F.E., Hartman, S.E., Westernströer, U., Küter, M., Benavides, R., da Silva, A.F., Bell, S., Payne, C., Olafsdottir, S., Robinson, K., Jantunen, L.M., Korablev, A., Webster, R.J., Jones, E. M., Gilg, O., Bailly du Bois, P., Beldowski, J., Ashjian, C., Yahia, N.D., Twining, B., Chen, X.-G., Tseng, L.-C., Hwang, J.-S., Dahms, H.-U., Oschlies, A., 2020. Global

variability in seawater Mg:Ca and Sr:Ca ratios in the modern ocean. Proc. Natl. Acad. Sci. 117, 22281–22292. https://doi.org/10.1073/pnas.1918943117.

Levi, A., Müller, W., Erez, J., 2019. Intrashell Variability of Trace elements in Benthic Foraminifera Grown under High CO2 Levels. Front. Earth Sci. 7.

Lewis, E.R., Wallace, D.W.R., 1998. Program developed for CO2 System Calculations (no. cdiac:CDIAC-105). In: Environmental System Science Data Infrastructure for a Virtual Ecosystem (ESS-DIVE) (United States). https://doi.org/10.15485/1464255.

Lorens, R.B., 1981. Sr, Cd, Mn and Co distribution coefficients in calcite as a function of calcite precipitation rate. Geochim. Cosmochim. Acta 45, 553–561. https://doi.org/10.1016/0016-7037(81)90188-5.

Lowenstein, T.K., Hönisch, B., 2012. The use of Mg/Ca as a Seawater Temperature Proxy. Paleontol. Soc. Pap. 18, 85–100. https://doi.org/10.1017/S1089332600002564.

Lueker, T.J., Dickson, A.G., Keeling, C.D., 2000. Ocean pCO2 calculated from dissolved inorganic carbon, alkalinity, and equations for K1 and K2: validation based on laboratory measurements of CO2 in gas and seawater at equilibrium. Mar. Chem. 70, 105–119. https://doi.org/10.1016/S0304-4203(00)00022-0.

Mackensen, A., Hald, M., 1988. Cassidulina teretis Tappan and C. laevigata d'Orbigny; their modern and late Quaternary distribution in northern seas. J. Foraminifer. Res. 18, 16–24. https://doi.org/10.2113/gsjfr.18.1.16.

Marchitto, T.M., Lynch-Stieglitz, J., Hemming, S.R., 2005. Deep Pacific CaCO3 compensation and glacial–interglacial atmospheric CO2. Earth Planet. Sci. Lett. 231, 317–336. https://doi.org/10.1016/j.epsl.2004.12.024.

Martínez-Botí, M.A., Foster, G.L., Chalk, T.B., Rohling, E.J., Sexton, P.F., Lunt, D.J., Pancost, R.D., Badger, M.P.S., Schmidt, D.N., 2015. Plio-Pleistocene climate sensitivity evaluated using high-resolution CO2 records. Nature 518, 49–54. https://doi.org/10.1038/nature14145.

McGrath, T., McGovern, E., Cave, R.R., Kivimäe, C., 2016. The Inorganic Carbon Chemistry in Coastal and Shelf Waters around Ireland. Estuar. Coasts 39, 27–39.

McIntyre-Wressnig, A., Bernhard, J.M., McCorkle, D.C., Hallock, P., 2013. Non-lethal effects of ocean acidification on the symbiont-bearing benthic foraminifer Amphistegina gibbosa. Mar. Ecol. Prog. Ser. 472, 45–60. https://doi.org/10.3354/meps09918.

McIntyre-Wressnig, A., Bernhard, J.M., Wit, J.C., Mccorkle, D.C., 2014. Ocean acidification not likely to affect the survival and fitness of two temperate benthic foraminiferal species: results from culture experiments. J. Foraminifer. Res. 44, 341–351. https://doi.org/10.2113/gsjfr.44.4.341.

Mewes, A., Langer, G., Reichart, G.-J., de Nooijer, L.J., Nehrke, G., Bijma, J., 2015. The impact of Mg contents on Sr partitioning in benthic foraminifers. Chem. Geol. 412, 92–98. https://doi.org/10.1016/j.chemgeo.2015.06.026.

Mezger, E.M., Nooijer, L.J., Boer, W., Brummer, G.J.A., Reichart, G.J., 2016. Salinity controls on Na incorporation in Red Sea planktonic foraminifera. Paleoceanography 31, 1562–1582. https://doi.org/10.1002/2016PA003052.

Mojtahid, M., Toucanne, S., Fentimen, R., Barras, C., Le Houedec, S., Soulet, G., Bourillet, J.-F., Michel, E., 2017. Changes in Northeast Atlantic hydrology during termination 1: Insights from Celtic margin's benthic foraminifera. Quat. Sci. Rev. 175, 45–59. https://doi.org/10.1016/j.quascirev.2017.09.003.

Mortyn, P.G., Elderfield, H., Anand, P., Greaves, M., 2005. An evaluation of controls on planktonic foraminiferal Sr/Ca: Comparison of water column and core-top data from a North Atlantic transect. Geochem. Geophys. Geosyst. 6 https://doi.org/10.1029/2005GC001047.

Murray, J.W., 1991. Ecology and Palaeoecology of Benthic Foraminifera. Longman Scientific and Technical.

Murray, J.W., 2006. Ecology and Applications of Benthic Foraminifera. Cambridge University Press.

Nardelli, M.P., Barras, C., Metzger, E., Mouret, A., Filipsson, H.L., Jorissen, F., Geslin, E., 2014. Experimental evidence for foraminiferal calcification under anoxia. Biogeosciences 11, 4029–4038. https://doi.org/10.5194/bg-11-4029-2014.

Nehrke, G., Reichart, G.J., Van Cappellen, P., Meile, C., Bijma, J., 2007. Dependence of calcite growth rate and Sr partitioning on solution stoichiometry: Non-Kossel crystal growth. Geochim. Cosmochim. Acta 71, 2240–2249. https://doi.org/10.1016/j.gca.2007.02.002.

Okai, T., Suzuki, A., Kawahata, H., Terashima, S., Imai, N., 2002. Preparation of a New Geological survey of Japan Geochemical Reference Material: Coral JCp-1. Geostand. Newslett. 26, 95–99. https://doi.org/10.1111/j.1751-908X.2002.tb00627.x.

Oron, S., Evans, D., Abramovich, S., Almogi-Labin, A., Erez, J., 2020. Differential sensitivity of a symbiont-bearing foraminifer to seawater carbonate chemistry in a decoupled DIC-pH experiment. J. Geophys. Res. Biogeosci. 125 https://doi.org/10.1029/2020JG005726 e2020JG005726.

Pascal, P.-Y., Dupuy, C., Richard, P., Niquil, N., 2008. Bacterivory in the common foraminifera Ammonia tepida: Isotope tracer experiment and the controlling factors. J. Exp. Mar. Biol. Ecol. 359, 55–61. https://doi.org/10.1016/j.jembe.2008.02.018.

Prazeres, M., Uthicke, S., Pandolfi, J.M., 2015. Ocean acidification induces biochemical and morphological changes in the calcification process of large benthic foraminifera. Proc. R. Soc. B Biol. Sci. 282, 20142782. https://doi.org/10.1098/rspb.2014.2782.

Qin, B., Jia, Q., Xiong, Z., Li, T., Algeo, T.J., Dang, H., 2022. Sustained deep Pacific carbon storage after the Mid-Pleistocene transition linked to enhanced Southern Ocean stratification. Geophys. Res. Lett. 49 https://doi.org/10.1029/2021GL097121 e2021GL097121.

Raitzsch, M., Dueñas-Bohórquez, A., Reichart, G.-J., de Nooijer, L.J., Bickert, T., 2010. Incorporation of Mg and Sr in calcite of cultured benthic foraminifera: impact of calcium concentration and associated calcite saturation state. Biogeosciences 7, 869–881. https://doi.org/10.5194/bg-7-869-2010.

Raitzsch, M., Kuhnert, H., Hathorne, E.C., Groeneveld, J., Bickert, T., 2011. U/Ca in benthic foraminifers: a proxy for the deep-sea carbonate saturation. Geochem. Geophys. Geosyst. 12 https://doi.org/10.1029/2010GC003344.

Rathburn, A.E., De Deckker, P., 1997. Magnesium and strontium compositions of recent benthic foraminifera from the Coral Sea, Australia and Prydz Bay, Antarctica. Mar. Micropaleontol. 32, 231–248. https://doi.org/10.1016/S0377-8398(97)00028-5.

Reichart, G.-J., Jorissen, F., Anschutz, P., Mason, P.R.D., 2003. Single foraminiferal test chemistry records the marine environment. Geology 31, 355–358. https://doi.org/10.1130/0091-7613(2003)031<0355:SFTCRT>2.0.CO;2.

Rheuban, J.E., Doney, S.C., McCorkle, D.C., Jakuba, R.W., 2019. Quantifying the effects of nutrient enrichment and freshwater mixing on coastal ocean acidification. J. Geophys. Res. Oceans 124, 9085–9100. https://doi.org/10.1029/2019JC015556.

Richter, F.M., Turekian, K.K., 1993. Simple models for the geochemical response of the ocean to climatic and tectonic forcing. Earth Planet. Sci. Lett. 119, 121–131. https://doi.org/10.1016/0012-821X(93)90010-7.

Roberts, J., Kaczmarek, K., Langer, G., Skinner, L.C., Bijma, J., Bradbury, H., Turchyn, A. V., Lamy, F., Misra, S., 2018. Lithium isotopic composition of benthic foraminifera: a new proxy for paleo-pH reconstruction. Geochim. Cosmochim. Acta 236, 336–350. https://doi.org/10.1016/j.gca.2018.02.038. Chemistry of oceans past and present: A Special Issue in tribute to Harry Elderfield.

Rosenthal, Y., Boyle, E.A., Slowey, N., 1997. Temperature control on the incorporation of magnesium, strontium, fluorine, and cadmium into benthic foraminiferal shells from Little Bahama Bank: prospects for thermocline paleoceanography. Geochim. Cosmochim. Acta 61, 3633–3643. https://doi.org/10.1016/S0016-7037(97)00181-6.

Rosenthal, Y., Lear, C.H., Oppo, D.W., Linsley, B.K., 2006. Temperature and carbonate ion effects on Mg/Ca and Sr/Ca ratios in benthic foraminifera: Aragonitic species Hoeglundina elegans. Paleoceanography 21, PA1007. https://doi.org/10.1029/2005PA001158.

Schneider, A., Crémière, A., Panieri, G., Lepland, A., Knies, J., 2017. Diagenetic alteration of benthic foraminifera from a methane seep site on Vestnesa Ridge (NW Svalbard). Deep Sea Res. Part Oceanogr. Res. 123, 22–34. https://doi.org/10.1016/j.dsr.2017.03.001.

Sexton, P.F., Wilson, P.A., Pearson, P.N., 2006. Microstructural and geochemical perspectives on planktic foraminiferal preservation: "Glassy" versus "Frosty". Geochem. Geophys. Geosyst. 7 https://doi.org/10.1029/2006GC001291.

Spearman, C., 1904. The proof and measurement of association between two things. Am. J. Psychol. 15, 72–101. https://doi.org/10.2307/1412159.

Stocker, T.F., Schmittner, A., 1997. Influence of CO_2 emission rates on the stability of the thermohaline circulation. Nature 388, 862–865. https://doi.org/10.1038/42224.

Tesoriero, A.J., Pankow, J.F., 1996. Solid solution partitioning of Sr^{2+}, Ba^{2+}, and Cd^{2+} to calcite. Geochim. Cosmochim. Acta 60, 1053–1063. https://doi.org/10.1016/0016-7037(95)00449-1.

Toyofuku, T., Kitazato, H., Kawahata, H., Tsuchiya, M., Nohara, M., 2000. Evaluation of Mg/Ca thermometry in foraminifera: Comparison of experimental results and measurements in nature. Paleoceanography 15, 456–464. https://doi.org/10.1029/1999PA000460.

Toyofuku, T., Suzuki, M., Suga, H., Sakai, S., Suzuki, A., Ishikawa, T., de Nooijer, L.J., Schiebel, R., Kawahata, H., Kitazato, H., 2011. Mg/Ca and δ^{18}O in the brackish shallow-water benthic foraminifer Ammonia 'beccarii.'. Mar. Micropaleontol. 78, 113–120. https://doi.org/10.1016/j.marmicro.2010.11.003.

Toyofuku, T., Matsuo, M.Y., de Nooijer, L.J., Nagai, Y., Kawada, S., Fujita, K., Reichart, G.-J., Nomaki, H., Tsuchiya, M., Sakaguchi, H., Kitazato, H., 2017. Proton pumping accompanies calcification in foraminifera. Nat. Commun. 8, 14145. https://doi.org/10.1038/ncomms14145.

van Dijk, I., de Nooijer, L.J., Reichart, G.-J., 2017a. Trends in element incorporation in hyaline and porcelaneous foraminifera as a function of pCO$_2$. Biogeosciences 14, 497–510. https://doi.org/10.5194/bg-14-497-2017.

van Dijk, I., de Nooijer, L.J., Wolthers, M., Reichart, G.-J., 2017b. Impacts of pH and [CO_3^{2-}] on the incorporation of Zn in foraminiferal calcite. Geochim. Cosmochim. Acta 197, 263–277. https://doi.org/10.1016/j.gca.2016.10.031.

van Dijk, I., Mouret, A., Cotte, M., Le Houedec, S., Oron, S., Reichart, G.-J., Reyes-Herrera, J., Filipsson, H.L., Barras, C., 2019. Chemical heterogeneity of Mg, Mn, Na, S, and Sr in benthic foraminiferal calcite. Front. Earth Sci. 7, 281. https://doi.org/10.3389/feart.2019.00281.

Van Marle, L.J., 1988. Bathymetric distribution of benthic foraminifera on the Australian-Irian Jaya continental margin, eastern Indonesia. Mar. Micropaleontol. 13, 97–152. https://doi.org/10.1016/0377-8398(88)90001-1.

Vigier, N., Rollion-Bard, C., Levenson, Y., Erez, J., 2015. Lithium isotopes in foraminifera shells as a novel proxy for the ocean dissolved inorganic carbon (DIC). Compt. Rendus Geosci. 347, 43–51. https://doi.org/10.1016/j.crte.2014.12.001.

Wakaki, S., Obata, H., Tazoe, H., Ishikawa, T., 2017. Precise and accurate analysis of deep and surface seawater Sr stable isotopic composition by double-spike thermal ionization mass spectrometry. Geochem. J. 51, 227–239. https://doi.org/10.2343/geochemj.2.0461.

Weinmann, A.E., Goldstein, S.T., Triantaphyllou, M.V., Langer, M.R., 2021. Community responses of intertidal foraminifera to pH variations: a culture experiment with propagules. Aquat. Ecol. 55, 309–325. https://doi.org/10.1007/s10452-021-09833-w.

Wit, J.C., 2012. Calibration, validation and application of foraminiferal carbonate based proxies. In: Reconstructing Temperature, Salinity and Sea Water Mg/Ca, LPP Contributions Series, 38. ed. Faculty of Geosciences, Utrecht University.

Wit, J.C., de Nooijer, L.J., Barras, C., Jorissen, F.J., Reichart, G.J., 2012. A reappraisal of the vital effect in cultured benthic foraminifer Bulimina marginata on Mg/Ca values: assessing temperature uncertainty relationships. Biogeosciences 9, 3693–3704. https://doi.org/10.5194/bg-9-3693-2012.

Wit, J.C., Davis, M.M., Mccorkle, D.C., Bernhard, J.M., 2016. A short-term survival experiment assessing impacts of ocean acidification and hypoxia on the benthic foraminifer Globobulimina turgida. J. Foraminifer. Res. 46, 25–33. https://doi.org/10.2113/gsjfr.46.1.25.

Wu, Y., Hain, M.P., Humphreys, M.P., Hartman, S., Tyrrell, T., 2019. What drives the latitudinal gradient in open-ocean surface dissolved inorganic carbon concentration? Biogeosciences 16, 2661–2681. https://doi.org/10.5194/bg-16-2661-2019.

Yu, J., Elderfield, H., Hönisch, B., 2007. B/Ca in planktonic foraminifera as a proxy for surface seawater pH. Paleoceanography 22. https://doi.org/10.1029/2006PA001347.

Yu, J., Elderfield, H., Piotrowski, A., 2008. Seawater carbonate ion-δ^{13}C systematics and application to glacial-interglacial North Atlantic Ocean circulation. Earth Planet. Sci. Lett. https://doi.org/10.1016/j.epsl.2008.04.010.

Yu, J., Foster, G.L., Elderfield, H., Broecker, W.S., Clark, E., 2010. An evaluation of benthic foraminiferal B/Ca and δ^{11}B for deep ocean carbonate ion and pH reconstructions. Earth Planet. Sci. Lett. 293, 114–120. https://doi.org/10.1016/j.epsl.2010.02.029.

Yu, J., Elderfield, H., Jin, Z., Tomascak, P., Rohling, E.J., 2014. Controls on Sr/ca in benthic foraminifera and implications for seawater Sr/Ca during the late Pleistocene. Quat. Sci. Rev. 98, 1–6.

Yu, Z., Lei, Y., Li, T., Zhang, S., Xiong, Z., 2019. Mg and Sr uptake in benthic foraminifera Ammonia aomoriensis based on culture and field studies. Palaeogeogr. Palaeoclimatol. Palaeoecol. 520, 229–239. https://doi.org/10.1016/j.palaeo.2019.02.001.

Zeebe, R.E., Tyrrell, T., 2019. History of carbonate ion concentration over the last 100 million years II: revised calculations and new data. Geochim. Cosmochim. Acta 257, 373–392. https://doi.org/10.1016/j.gca.2019.02.041.

Zeebe, R.E, Wolf-Gladrow, D., 2001. CO_2 in Seawater: Equilibrium, Kinetics, Isotopes, 65. Elsevier Oceanography Series.